2007

ORIENTATION-SPECIFIC IMMOBILIZATION OF BMP-2 ON PLGA SCAFFOLDS

Randall K. Hilliard
University of Kentucky, rhilliard@rtix.com

ABSTRACT OF THESIS

ORIENTATION-SPECIFIC IMMOBILIZATION OF BMP-2 ON PLGA SCAFFOLDS

A variety of synthetic bone graft materials such as the polymer poly(lactic-co-glycolic acid) (PLGA) have been investigated as alternatives to current tissue based bone graft materials. In this study, efforts have been made to improve the tissue-PLGA interface by immobilizing bone morphogenetic protein-2 (BMP-2) in an oriented manner on scaffolds using covalently immobilized heparin. The results demonstrated a four-fold increase in covalently immobilized heparin compared to non-specific heparin attachment. Furthermore, the scaffolds with covalently attached heparin retained approximately three-fold more BMP-2 than did either scaffolds with no heparin attached or scaffolds with non-specific heparin attachment. The activity of scaffolds with BMP-2 immobilized in various manners was examined using an alkaline phosphatase assay on C3H10T1/2-seeded scaffolds. These results indicated approximately twice the amount of activity with scaffolds that had BMP-2 immobilized with covalently attached heparin than on scaffolds with adsorption of BMP-2 and a three-fold increase in activity when compared to scaffolds that had non-specific heparin attachment as the mechanism for BMP-2 immobilization. These results demonstrated that PLGA with covalently linked heparin has potential to immobilize BMP-2 in a specific orientation that is favorable for cell-receptor binding, leading to the more efficient use of the bone-growth factor.

KEYWORDS: PLGA, heparin, BMP-2, scaffolds, surface modification

Randall K. Hilliard
24 July 2007

ORIENTATION-SPECIFIC IMMOBILIZATION OF BMP-2 ON PLGA SCAFFOLDS

By

Randall K. Hilliard

David A. Puleo
Director of Thesis

Abhijit Patwardhan
Director of Graduate Studies

24 July 2007

RULES FOR USE OF THESIS

Name   Date

_____

_____

_____

_____

_____

_____

_____

_____

_____

_____

Thesis

Randall K. Hilliard

The Graduate School

University of Kentucky

2007

ORIENTATION-SPECIFIC IMMOBILIZATION OF BMP-2 ON PLGA SCAFFOLDS

_____

THESIS

_____

A thesis submitted in partial fulfillment of the requirements
for the degree of Master of Science in Biomedical Engineering
in the Graduate school at the University of Kentucky

By

Randall K. Hilliard

Lexington, Kentucky

Director: Dr. David A. Puleo, Professor of Biomedical Engineering

Lexington, Kentucky

2007

MASTER'S THESIS RELEASE

I Authorize the University of Kentucky
Libraries to reproduce this thesis in
Whole or in part for purposes of research

Randy Hilliard

24 July 2007

ACKNOWLEDGEMENTS

TABLE OF CONTENTS

LIST OF TABLES

LIST OF FIGURES

1   INTRODUCTION

Bone defects, regardless of whether occurring due to trauma or to disease, that are too large to repair on their own typically require bone grafts for the healing process. One of the most popular current bone graft techniques is the use of autografts whereby bone tissue is surgically removed from one location on the patient, and then implanted into the defect. The advantage associated with autografts is the compatibility of the tissue. Because the implanted material comes from the host, there is no risk for disease transmission. However this method requires one surgery to harvest the bone tissue and another to implant it at the defect site. Supply and donor site morbidity are also problems associated with autografts.

Allografts are another option. Here the bone tissue comes from same species' donors in the form of demineralized bone matrix particles, or a combination of cancellous and cortical bone chips and paste. Allografts do well at providing a natural tissue matrix for bone regeneration, but like autografts, donor tissue can be scarce. Also, there is a risk for disease transmission and the potential for an adverse immune response.

Xenografts are yet another option for bone grafts. With xenografts, the bone tissue used in the grafting process is usually bovine or porcine in origin, which could address the lack of donor tissue. However, there is still the risk of disease transmission and the added potential for an adverse immune response similar to allograft tissue.

Synthetic bone graft substitutes are an option that is growing in popularity. Synthetic materials range from ceramics, such as calcium sulfate and calcium phosphate, to polymers, such as poly(lactic-co-glycolic) acid (PLGA) and the biopolymer chitosan. Synthetics have the potential to provide a virtually unlimited supply of graft material.

They also only require one surgery for graft procedure as there is no need to surgically remove tissue from a donor site. Disease transmission would be minimized as well.

Another advantage of synthetics as bone graft alternatives is that they can be modified to improve biocompatibility. Growth factors and other biomolecules can be immobilized on the biomaterial surface to generate a specific desired response. For bone grafts, the ideal response would be that the implanted material would induce bone regeneration such that native bone tissue from the host grows into the defect site.

A variety of methods exist to link the growth factors to the polymer. They can be directly adsorbed on the surface or chemically attached at specific locations. Alternatively, another compound can be used to link the polymer with the growth factor in such a way that the growth factor is oriented in a particular manner. The advantages of chemically attaching the biomolecules to the surface are that stability of binding is increased with covalent attachment and the orientation can be better controlled than with random adsorption. The surface density of the biomolecules has potential to be controlled using direct chemical attachment as well. Using a chemical spacer can have the same advantages as direct attachment and can reduce steric hindrance of the biomolecule by getting it away from the biomaterial surface, potentially increasing its effectiveness at generating the desired biological response.

Based on the above knowledge, we hypothesized that the oriented attachment of the growth factor bone morphogenetic protein 2 (BMP-2) to PLGA scaffolds would lead to a better cellular response *in vitro* than the random adsorption or even random covalent immobilization of BMP-2 on the scaffolds. It is expected that future *in vivo* studies

2

examining oriented growth factor attachment to polymer scaffolds would show a

regeneration response of the host bone tissue instead of just a repair response.

2 BACKGROUND AND SIGNIFICANCE

2.1 Biomaterials

In 2005 there were more than 500,000 bone graft procedures done in the United States and 2.2 million done world-wide.[1] With the aging of the U.S. population one can expect those numbers to increase. Of the different tissue-based bone grafting techniques, autografts are considered the gold standard.[1, 2] However, all have disadvantages. Autografts require one surgery on the same patient to harvest the bone, typically from the iliac crest, and then another to implant the bone tissue at the defect site. Allografts and xenografts have the risk of disease transmission. Autografts and allografts have problems associated with supply. All three types have some potential for infection and adverse immune responses. With the faults of the current tissue-based grafting techniques and the obvious need for bone graft materials, efforts have been made to use tissue engineering approaches to improve upon those techniques and materials.[2-8]

Tissue engineering is a concept whereby the biomaterial is either seeded with living cells before implantation (the *in vitro* approach) or designed to attract cells upon implantation (the *in vivo* approach).[9] The cells, using the scaffolds as a mechanical support, then proliferate and differentiate and generally become metabolically active with the production of extracellular matrix.[8, 9] The cells continue to become more bioactive and show signs of organization. Concurrently, the degradation of the scaffold is also occurring with the newly regenerated tissue replacing the artificial biomaterial.[8, 9] With regards to bone tissue engineering, the overall goal is to use the biomaterial to generate a specific set of receptor-ligand responses instead of relying upon non-specific interactions to cause the regeneration of natural, healthy, native bone tissue.[10]

4

Ideally, the tissue engineering approach would lead to a bone graft material that induces a regenerative response of the host bone tissue in addition to repairing the defect site.[9] To do this, the bone graft material would need to be osteoconductive in that it would provide a conduit for the growth and expansion of the host bone tissue into the graft material that occupies the defect site. It should also be osteoinductive, in that it would activate host osteoprogenitor cells in the surrounding tissue to induce the formation of new bone that would serve to fill the defect site as the graft material biodegrades. The capacity to be osteogenic, meaning to have cells capable of proliferating and differentiating to osteoblasts, is also desirable.

Given the concept of tissue engineering and the limitations of natural tissue based bone grafts, a variety of synthetic alternatives have been developed or are being investigated for use as bone substitutes. Ceramics, such as calcium sulfates, calcium phosphates, and hydroxyapatite, have properties similar to the mineral of bone, but are neither osteoinductive nor osteogenic.[1] Another material of recent interest is the biopolymer, chitosan. It has been shown to have good biocompatibility, can be shaped easily to match the defect site, and can induce hard-tissue mineralization.[11] Other polymers and polymer blends are also being investigated. Of these, arguably the polymer generating the most interest as a potential bone graft biomaterial is poly(lactic-co-glycolic acid) (PLGA).

PLGA (Figure 2.1) is a biodegradable, random copolymer of varying ratios of poly(lactic acid) (PLA) and poly(glycolic acid) (PGA). It has been FDA approved for over 30 years for a variety of applications ranging from orthopedic devices to drug delivery systems.[2] It is also available commercially in a variety of molecular

weights.[2] The polymerization of PLGA usually occurs by combining ring opening

reactions of lactides and glycolides.
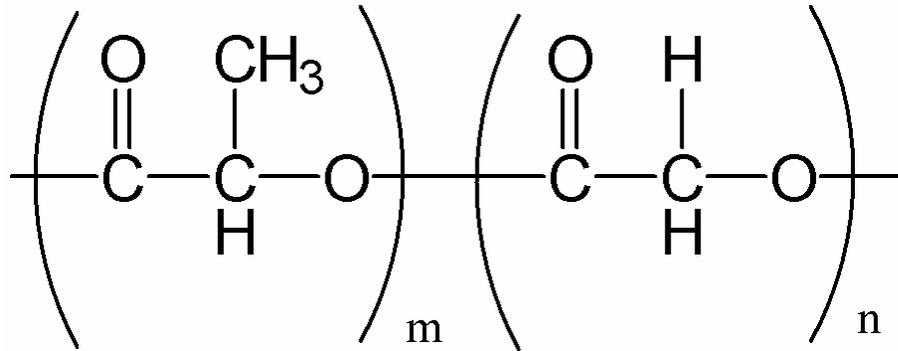
Figure 2.1: PLGA with lactic acid monomer (m) and glycolic acid monomer (n).

Many of the properties, such as crystallinity, degradation, and strength of PLGA,

can be controlled by varying the ratio of lactic acid to glycolic acid and also by changing

the molecular weight.[2] Typically, PLGA does not exceed 50% glycolic acid content.

This is primarily due to the degradation rate of PLGA being a function of the glycolic

acid content, with higher ratios of glycolic acid leading to faster degradation rates.

However, PGA is considered to have high crystallinity at ~ 50% [5, 12] and using more

than 50 % PGA can lead to crystalline regions that affect the mechanical properties of

PLGA.[8] Another note concerning degradation of PLGA is that its products are

naturally occurring compounds, lactic acid and glycolic acid. Both are easily

metabolized by the body, but can produce localized areas of high acid content if the

vascularization is poor in that area.[8]

With respect to crystallinity, both PLA and PGA can be crystalline and have high

moduli.[5, 12] As previously mentioned, PGA is highly crystalline. In contrast, PLA is a

chiral compound, with both the D- and L-PLA being highly crystalline, but the racemic

mixture of the two being amorphous. L-PLA crystallinity can reach 70%.[13] When

PGA and PLA are combined to form the copolymer PLGA, much of the crystallinity, and therefore much of the mechanical strength is lost. How much mechanical strength is lost is dependent upon the ratios of PLA to PGA and the chiral form of PLA.[14] As a general rule, mechanical strength and degradation resistance are directly proportional to PLGA crystallinity. Increasing the molecular weight of the PLGA chains can also result in increased compressive strength and modulus.[12]

Commercially available PLGA can be purchased with different terminal ends, such as carboxyl groups and hydroxyl groups. Other research groups have made amine-terminated PLGA as well.[15-17] The different chemical functional groups on the ends of the PLGA chains allow for a variety of surface modifications to be made to PLGA. These surface modifications can be used to tailor the properties of the PLGA surface for the desired use.

Another advantageous property associated with PLGA is its formability. Numerous studies have cited a variety of fabrication methods for creating porous PLGA scaffolds that provide an osteoconductive template for the growth of bone tissue.[2, 4, 6, 14, 15, 18-20] The unifying theme in all these studies is the creation of a porous scaffold with pore sizes suitable for penetration of cells into the scaffold with adequate mechanical properties to provide a support system for cell growth while accommodating degradation rates creating room for cell expansion. There have been a variety of methods used to fabricate these scaffolds, including solution-casting, salt-leaching, gas-foaming, and approaches involving the use of microspheres.[2, 4, 6, 14, 15, 18-23] These methods can produce scaffolds with a wide range or porosities and mechanical properties with higher porosity scaffolds having lower mechanical strength than lower porosity

scaffolds.[2] Each of the methods listed above, with the exception of the sintered

microsphere approach, require the extraction of a chemical or compound to produce

pores in the PLGA structure. In the case of salt-leaching, salt particles can become

trapped in the polymer scaffold resulting in poor interconnectivity of the pores.[2, 6]

Other phase separation techniques can result in small pore diameters that limit the

penetration of cells and tissue into the scaffolds.[2] It has been shown, that to get good

penetration of cells into the biomaterial, the pore diameters should be in the range of 100

- 250 μm.[2, 24]

In contrast to the above mentioned methods, the sintering of PLGA microspheres

can produce scaffolds that have pore sizes suitable for cell and tissue penetration along

with mechanical properties similar to that of trabecular bone.[2, 7] The "sintered

microsphere" approach involves the fusion of adjacent, similarly sized microspheres at

the glass transition temperature (T_g). The result of this approach is a scaffold with near

100% interconnectivity of the pores without the potential for other compounds to be

trapped within the scaffold.[2, 7]

2.2   Immobilization of Growth Factors

It is now known that porous, biodegradable scaffolds can be fabricated to serve as

a temporary extracellular matrix for tissue engineering applications. It is also known that

high porosities with large, interconnected pores are useful for the integration of cells and

tissue with the temporary extracellular matrix.[23, 25] While these studies have shown

limited success, there are additional efforts that have been made to improve

biocompatibility and regenerative capacity of these scaffolds. This work has largely

involved immobilizing growth factors on the polymer scaffolds, though, there have been

efforts to develop growth factor delivery systems.[3, 25] These systems could encompass gene, cell, or protein therapy methods. [25-27]

The immobilization of growth factors can provide an improved interaction between the host cells and tissue and the biomaterials that are implanted, thereby stimulating cellular activity. There are two general classes of immobilization techniques. The first being the simple adsorption of growth factors on the surface of the biomaterial. Certainly, growth factors and a variety of proteins will adsorb to the surface of the biomaterial upon implantation.[8] However, this is truly random adsorption in that the interaction between the implant and the host tissue is completely uncontrolled and dependent upon which molecules happen to be near at the time of implantation. A better approach would be to design an immobilization scheme that promotes a specific, controlled interaction between the implant and the host tissue. To accomplish this, some have attempted to adsorb specific biomolecules on the surface by dipping the device in the solution containing the molecule or molecules of interest.[28, 29] This process has shown some success, however since these molecules are held by weak interactions, many of the molecules will diffuse from the surface without eliciting the desired response.

The second immobilization technique is to chemically attach the biomolecules to the surface of the scaffold or implant before implantation. Some are examining the chemical attachment of small peptides, such as Arg-Gly-Asp (RGD) containing peptides, to the surface of the biomaterial as a way to promote cell attachment.[3, 30-32] The problem with using the RGD peptides are that many cell types have receptors capable of binding that peptide sequence. This would lead to non-specific attachment of cells.

Therefore, there are efforts underway to examine peptides that may be more specific for bone cells.[30-34]

While the chemical attachment of peptides could lead to a specific response such that the implant induces regenerative bone tissue, there is still the concern of a lack of specificity of the peptides for the bone cells. Chemically attaching proteins instead of peptides to the biomaterial surface would provide the mechanism to enhance bioactivity from the cells. Whereas immobilized peptides on the surface of a biomaterial could lead to improved cell attachment, the immobilization of whole proteins could lead to improved cell attachment and to increased cellular function and differentiation. Furthermore, the immobilization of a particular type of protein or proteins would be more likely to produce specific receptor-ligand interactions that could be used to produce a desired outcome. This method of attachment is essentially immobilizing growth factors in a manner similar to the way they would be immobilized in the extracellular matrix.

Another advantage of chemically attaching whole proteins or growth factors to the biomaterial surface is that the growth factor can be immobilized in a specific orientation. Care must be taken to minimize covalent attachment of the growth factors to the biomaterial in locations that would otherwise be used to bind to cell receptors. However, if oriented immobilization can be achieved, then the growth factor can be oriented such that the cell-receptor binding region is in the optimal position to interact with cell receptors. Positioning the growth factors on the biomaterial in that manner could lead to more effective integration of the biomaterial and, therefore, to an enhanced regeneration response for the host bone tissue.

Figure 2.2 shows a cartoon comparing the random attachment of growth factors on the surface of a biomaterial to the oriented attachment of growth factors. This demonstrates how with oriented attachment, all the cell-receptor binding regions are in the optimal position for interaction with the cell receptor. In contrast, with random attachment of growth factors, there is no certainty that the cell-receptor binding region will be in a position where it can bind with cell receptors, and is obviously an inefficient use of the growth factors.
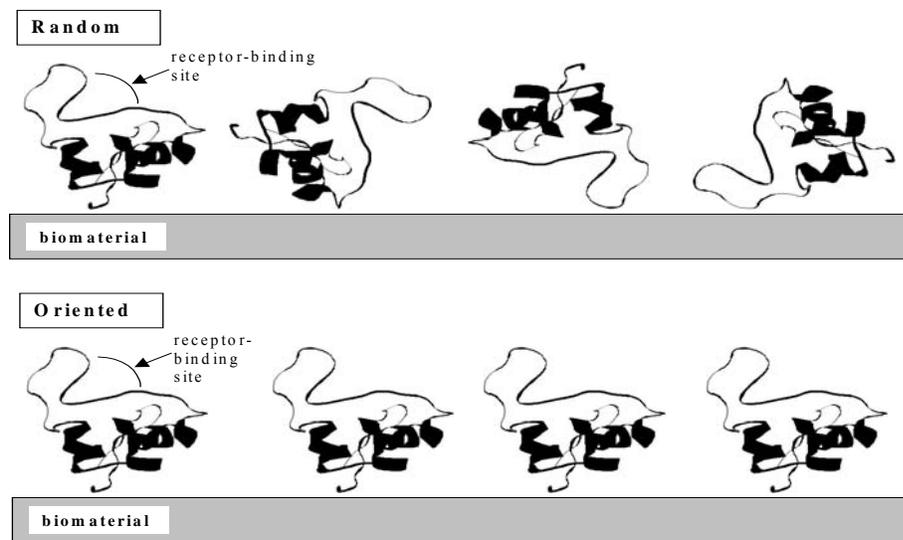
Figure 2.2: Random versus oriented immobilization of growth factors

2.3 Bone Morphogenetic Protein 2 (BMP-2)

For this research, the biomaterial of interest was PLGA and the growth factor of choice was BMP-2. Part of the reason for choosing PLGA was that the ends of the polymer chains can have a variety of chemical functional groups that can provide ideal locations to immobilize growth factors. BMP-2 was used as the growth factor because of its role in inducing differentiation of osteoprogenitor cells to osteoblasts.[25, 35]

BMPs were first identified when implanted demineralized bone matrix (DBM) was observed to induce ectopic bone formation in rodents [25, 27, 36, 37] and are part of the transforming growth factor-β family (TGF-β). BMP-2, a member of the BMP family, is a homodimer consisting of two, 114 amino acid chains that are connected by seven disulfide bonds, which are a prerequisite for bone induction.[35, 36, 38, 39] The molecular weight of the BMP-2 monomer has been reported to be approximately 12,000 - 14,000 Da.[38] In addition to the differentiation of osteoprogenitor cells to osteoblasts, human recombinant BMP-2 (rhBMP-2) has shown osteoinductive effects on C3H10T1/2 mouse pluripotent cells.[36] Furthermore, experiments have shown an increase in osteoblastic parameters in human bone marrow such that osteoblast precursor cells were induced to differentiate into osteoblasts.[36, 40] Experiments have also shown that BMP-2 does not stimulate mature osteoblasts or fibroblasts.[40] This indicates that the osteogenic effects of BMP-2 are directed towards multipotent or pluripotent cells such as mesenchymal stem cells that can differentiate to chondrocytes and osteoblasts that develop cartilage and bone.[1, 10, 15, 25, 27, 35-37, 40-49] BMPs have also been linked with accelerated fracture repair and have been shown to promote spinal fusions in *in vivo* experiments.[25, 36, 46]

BMP-2 interacts with cells via a complex of two types of serine/threonine-kinase receptor chains. BMP receptor-IA (BRIA) and BMP receptor-IB (BRIB) are the type I receptors. These are considered the high affinity receptors for BMP-2.[38, 50-54] BMP-receptor-II (BRII) is the second type (type II) and is considered the low affinity receptor. [38, 50, 52, 53, 55] Once BMP-2 binds with the receptor, the BRII receptor phosphorylates the type I receptors which then phosphorylates a Smad intracellular

protein. This phosphorylation sequence triggers the activation of other Smad proteins that eventually lead to gene transcription.[36, 49, 50, 55] The interaction of BMP-2 with BRIA (Figure 2.3) involves both BMP-2 monomers and consists of a mostly hydrophobic contact area.[51-53] Figure 2.3 shows a top-down view of the BMP-2:BRIA complex. The BMP monomers are in gold and blue with the receptors shown in green. The chain termini are identified with "N's" and "C's" that represent the amino-terminus and the carboxyl terminus, respectively. The "wrist" and "knuckle" epitopes refer to binding regions for BRIA and BRII, respectively.[51-53] It is important to note that the receptor binding epitopes on BMP-2 do not include either N-terminus of the protein. This implies that the N-terminus region of BMP-2 is an effective location for use in immobilizing the growth factor in a specific orientation to the biomaterial, PLGA.
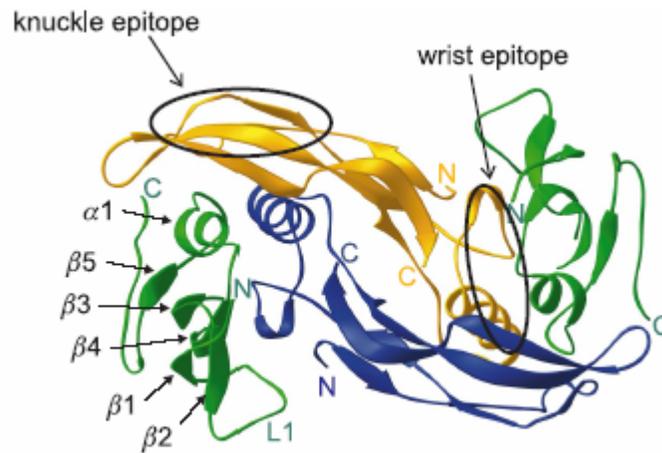
Figure 2.3: Top-down view of BMP-2 (gold and blue portion) binding with BRIA receptor (green portion)[51] (See text for detailed description)

2.4   Methods to Link and Orient BMP-2 to PLGA Scaffolds

Given the promising potential of the N-terminus of BMP-2 as a location for immobilizing and orienting the growth factor on the polymer, the manner in which the BMP-2 will be immobilized needs to be determined. Certainly, the BMP-2 can be immobilized directly to the carboxyl groups of the PLGA chains. However, there are reports that an optimal density of growth factors may exist for inducing a preferred cellular response.[32, 56, 57] It is also known that the distance between the immobilized growth factor and the biomaterial surface can noticeably affect the activity of the growth factor.[58, 59] In efforts to link BMP-2 to the PLGA scaffolds, chemical spacers could be used to control both the surface density of the BMP-2, as well as the distance from the PLGA substrate (Figure 2.4). Regarding surface density of the spacer, an initial consideration may be to immobilize as many growth factors as possible such that they are packed tightly together. However close proximity of the molecules may actually prevent or hinder the ability of the molecules to interact with the cell receptors simply because there would not be enough room between each individual BMP-2 molecule. In a similar manner, the spacer could also be used to control the distance between the growth factor and the biomaterial surface. If BMP-2 is too close to the surface, steric hindrance effects could reduce the ability of BMP-2 to bind with the receptor. The use of a spacer that is too long could also lead to poor interaction between BMP-2 and the receptor due to the spacer lacking the rigidity to hold the growth factor in place.
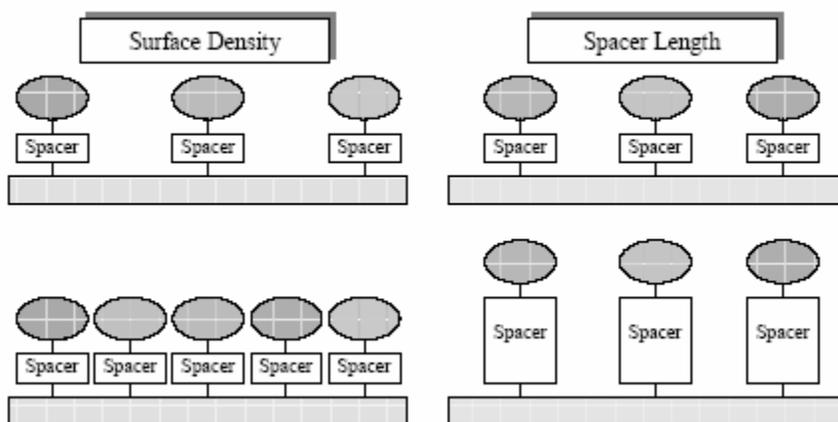
Figure 2.4: Illustration depicting the use of spacers to control surface density (left) and distance from substrate (right) of growth factors on biomaterial

2.4.1 Dihydrazides as Spacers

Two different compounds were considered for use as spacers for this research. The first compounds chosen were dihydrazides. Dihydrazides are symmetrical molecules that can have multiple methyl groups (CH_2) located between two hydrazide functional groups (Figure 2.4.1). The symmetry associated with dihydrazides suggests there is no need to use a blocking group on one end of the compound, while the other end is attached to the polymer surface. Linking the dihydrazide to the biomaterial can be accomplished using simple carbodiimide chemistry.[60] Another advantage of using dihydrazides as a spacer between the PLGA scaffolds and the BMP-2 is that the distance between polymer and growth factor can be easily manipulated by the addition or subtraction of methyl groups between the hydrazide functional groups.
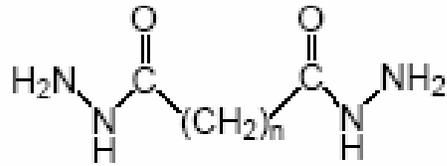
Figure 2.4.1: General dihydrazide structure

2.4.2 Heparin as a Spacer Molecule

Heparin is a highly sulfated, extracellular matrix glycosaminoglycan (GAG) that has high potential as an effective spacer molecule. Numerous studies have highlighted the enhancing effects of heparin on BMPs, other members of the TGF-β family, and growth factors in general.[15, 16, 35, 45, 48, 61-63] One of the suggested mechanisms used by heparin to enhance BMP-2 bioactivity is its ability to bind the polypeptide noggin and prevent it from interacting with BMP-2.[15, 45, 62] Noggin is an inhibitor of BMP-2 and the binding of noggin by heparin prevents its antagonistic ability on BMP-2.[15, 45, 49, 62] Heparin is also associated with retaining BMP-2 activity, preventing its degradation and increasing the half-life by 20-fold.[15, 45]

There is also evidence to suggest that heparin binds BMP-2 at the N-terminus region.[38, 48, 54] This suggests that part of the reason for the increase in activity of BMP-2 is that heparin does not interfere with the cell-receptor binding regions of the growth factor. It also further supports that immobilizing BMP-2 by binding the N-terminus of the protein is an effective way of orienting the growth factor to induce maximum cellular activity.

While numerous studies have examined the effects of heparin on BMP-2, only one study looked at the effects of heparin-conjugated PLGA scaffolds on the activity of

16

BMP-2.[15] The results of that study suggested that BMP-2 delivery could be sustained for a longer period with PLGA scaffolds that were conjugated with heparin as opposed to scaffolds with no heparin. Their experiment used amine-terminated PLGA that was synthesized in their lab by using the ring-opening polymerization of PLA and PGA. They also used carbodiimide chemistry to link the carboxyl groups on heparin to the amine-terminated PLGA. This is in contrast to our study which looked at immobilizing the heparin on the PLGA scaffolds by creating an ester bond between the hydroxyl groups on heparin and the carboxyl group on the PLGA chains.

2.5   Significance

One could expect ever increasing incidences of trauma and bone disease as the U.S. population continues to age. This will require a corresponding need for improved products for orthopedic care. With regards to bone grafting techniques and materials, the current gold standard of treatment is the autograft, although allografts and xenografts are also options. Given that no native graft and grafting procedure is without fault, there is a growing need for viable synthetic bone grafting biomaterials. The immobilization of growth factors and other biomolecules on a bone graft biomaterial has the potential to improve the integration of that material with the host tissue. If the proper types of biomolecules are immobilized, then the integration of the biomaterial could lead to a regenerative response, whereby host bone tissue is created in the defect site resulting in natural, healthy bone. The bioactivity of the material could be further increased if the immobilization of the biomolecules occur in an oriented manner where the cell-receptor binding region is positioned for binding with cell-receptors. Certainly, another advantage of presenting the biomolecules in an oriented manner is efficiency. Random

immobilization of biomolecules on a biomaterial surface may or may not result in

molecules that are oriented in an effective manner, increasing the likelihood of wasted

space and molecules.

3   METHODS AND MATERIALS

3.1   Polymer

The polymer used in this investigation was poly(lactic-co-glycolic acid) (PLGA) obtained from Absorbable Polymers (Pelham, AL). It is a random copolymer with a 50:50 ratio of lactic acid to glycolic acid and has carboxylic acid groups on the ends of the chains. The molecular weight was approximately 9-23.2 kDa based on inherent viscosity data, and its glass transition temperature (T_g) was 42-44°C.

3.1.1   PLGA on Coverslips

An 11.76% (w/v) solution of PLGA was made by adding 1.0 g of PLGA to 8.5 ml of dichloromethane (Sigma-Aldrich, St. Louis, MO). The solution was vortexed until the polymer dissolved and then sonicated at 25 W for an additional 30 s. The dissolved PLGA solution was added dropwise to coverslips (12 mm diameter, Fisher Scientific) until coated. Usually 4 to 5 drops per coverslip were sufficient to coat them. The PLGA coated coverslips were then allowed to air dry for approximately 15 min and then put under vacuum until used.

3.1.2   PLGA coated Test Tubes

PLGA-coated glass test tubes (Fisher, 12 by 75 mm) were prepared in a similar manner to the coverslips, with the difference being that 70 μl of the 11.76% (w/v) polymer solution was added to each test tube. The tubes were left under the hood to allow for the solvent to evaporate, leaving behind the PLGA coated test tubes. The

volume of PLGA solution used was based on covering the rounded bottom portion of the test tube.

3.1.3 Microspheres

Polyvinyl alcohol (PVA) (Sigma) was added to deionized-water (6.0 g in 600 ml). While the PVA was dissolving in the deionized-water, a 11.76% (w/v) solution of PLGA in dichloromethane was prepared by dissolving 800 mg of PLGA in 6.8 ml of dichloromethane then sonicating at 25 W for 90 seconds. Once the PVA and PLGA were both in solution, the PLGA solution was added dropwise using a pasteur pipet to the PVA solution while it was being stirred using a magnetic stir bar and stir plate at 600 rpm to create an oil-in-water emulsion. Care was taken to add the PLGA directly to the bottom of the PVA solution vortex to ensure the resulting PLGA microspheres were not too large. The resulting suspension of microspheres was kept spinning at 600 rpm overnight to ensure that the dichloromethane solvent completely evaporated. The PLGA microspheres were isolated using vacuum filtration with P4 filter paper (Fisher). The microspheres were rinsed with deionized-water thoroughly and then allowed to remain under vacuum for another 15 min. Finally, the microspheres were placed in a desiccator under vacuum until used.

The first modification to the previously mentioned microsphere procedure was to use centrifugation to recover the microspheres from suspension instead of vacuum filtration. For this procedure, the PLGA/PVA emulsion was prepared exactly as mentioned above. After the PLGA/PVA emulsion had spun overnight, the stirrer was turned off and the PLGA microspheres were allowed to settle in the beaker for 2-3 h. Next, the supernatant was removed, and the remaining microspheres were rinsed into a

50 ml centrifuge tube. The microspheres were then centrifuged at 1500g for 10 minutes

followed by the removal of the supernatant. The microspheres were then resuspended in

deionized-water and centrifuged again for 10 min. This was repeated twice. Following

the three rinses, the microspheres were frozen at -70°C overnight then lyophilized for 24

h, and stored under vacuum at room temperature with desiccant until further use.

A further modification in the making of the microspheres was also used. For this

modification, the dissolved PLGA was added to the PVA solution while using a

homogenizer (Omni PDH) to ensure uniformity in microsphere size. Microspheres were

made using the homogenizer at speeds of 5500 rpm and 1500 rpm for three minutes.

The final modification to the microsphere preparation procedure involved the

addition of the dissolved PLGA solution to the PVA solution using a pasteur pipet as

mentioned above. This time, the magnetic stirrer was set to 450 rpm and the dissolved

PLGA was added rapidly (instead of dropwise) to the outer edge of the vortex (instead of

to the bottom of the vortex) and allowed to stir overnight. The resulting microspheres

were isolated by using vacuum filtration, then frozen overnight at -70°C before

lyophilizing for 24 h. Microspheres were then stored under vacuum at room temperature

with desiccant until use.

3.1.4   PLGA Scaffolds

PLGA scaffolds were prepared based on the sintered microsphere approach.[2, 6,

7] Scaffold preparation began by using a mortar and pestle to gently break up the

clumped microspheres. The microspheres were then sieved to isolate the microspheres

with diameters of 50 - 150 microns. Microspheres with diameters greater than 150

microns were also kept. Initially all scaffolds were made by pouring 25 mg of the 50-150

micron microspheres into a mold having cylindrical holes that were 5 mm wide and 6 mm deep and then heating at T_g (~ 43°C) for 24 h. Heating at this temperature served to fuse the microspheres together without completely melting them into one solid mass. The fused microspheres created an interconnected porous scaffold.

A modification of this procedure for making scaffolds was to pour the loose microspheres into the mold, taking care to completely fill all the mold holes with microspheres, then giving the mold a gentle tap to settle the microspheres before placing in the oven at T_g for 24 h. This version of the procedure was much less tedious to perform, and it resulted in larger scaffolds with less variability in the shape of the cylinder. After 24 h, the scaffolds were allowed to cool to room temperature before being removed from the mold. The scaffolds were stored in a freezer in a desiccator until used.

3.2   Material Characterization

3.2.1   Particle Size Testing

Particle size testing was accomplished using a Horiba Partica LA-950 laser scattering particle size distribution analyzer. Briefly, the procedure involved suspending approximately 0.5 g of the PLGA microspheres in deionized water then pipetting the suspension into the inlet on the machine. This was done to determine the range and distribution of the microspheres prepared by the various methods mentioned above before the microspheres were sieved for use in scaffold construction.

3.2.2 Porosity

The PLGA scaffolds made by sintering 25 mg of 50-150 micron diameter microspheres together were characterized by mercury intrusion porisometry (MIP) using a Micromeritics AutoPore IV 9500. Percent porosity and pore size distribution were provided in the output from the equipment. To determine the surface area of the scaffolds, the mass of the sample used was multiplied by the total pore area (m^2/g) to give total area. This area was divided by the total number of scaffolds used to get surface area per scaffold.

3.2.3 Scanning Electron Microscopy (SEM)

Initial scaffolds (25 mg) were mounted on an SEM stub using colloidal graphite (Ted Pella, Inc. Redding, CA). Each stub underwent gold sputter coating in an argon atmosphere using the Emscope sc 400. The samples were then viewed using a Hitachi S-3200 (Tokyo, Japan) with an accelerating voltage of 5kV. Scaffolds that were made by filling the entire mold with PLGA microspheres were prepared in a similar manner to the previously mentioned scaffolds, but were viewed using a Hitachi S-2700 SEM-EDX (Tokyo, Japan). In both cases, SEM pictures were taken of the surface and of cross-sections of the scaffolds.

3.2.4 Mechanical Testing of Scaffolds

Compressive strength and modulus were determined for the scaffolds made by pouring microspheres into the mold using a Bose Electroforce 3300 Mechanical Testing System with WinTest 3.0 software. Testing was conducted under displacement control using a 50 lb (222.5 N) load cell. Once the system was calibrated/tared and the crosshead

was in the correct position, the samples were loaded to failure utilizing compression platens. Testing was done at a rate of 1 mm/minute. The data was converted to Microsoft Excel format then and the force-displacement data was converted to stress-strain curves. Strain was determined from the values for displacement and the original height of the scaffolds. The slope of the initial linear portion of the stress-strain curve was then used to determine the modulus. The compressive strength was estimated by determining the stress just after the initial linear portion of the stress-strain curve.

3.3   Surface Modification

All surface modification attempts were based on using the free carboxyl group at the end of the polymer chains to attach either dihydrazides of multiple carbon chain lengths or to attach heparin. The chemistry used to attach the spacers and the quantification methods are discussed in the following sections.

3.3.1   Hydrazides

The hydrazide groups on either end of the dihydrazides make the compounds ideal for linking proteins and other bone growth factors to the PLGA backbone. Four different dihydrazides were used. They were oxalic dihydrazide (Alfa Aesar), succinic dihydrazide (Aldrich), adipic dihydrazide (Sigma), and sebacic dihydrazide (TCI America). See Figure 3.3.1a for the structures.

Figure 3.3.1a: Dihydrazide structures

To get the dihydrazides to react with the carboxyl groups of the PLGA, they were first dissolved in 0.1 M 2-(N-morpholino)ethanesulfonic acid (MES) (Sigma), pH 6.0. To activate the surface of the PLGA backbone for attachment of the dihydrazides, a 0.067 mM solution of 1-ethyl-3-(3-dimethylaminopropyl)-carbodiimide hydrochloride (EDAC) (Sigma) and 0.027 mM N-hydroxysuccinimide (NHS) (Fluka) was used (see Figure 3.3.1b). Each PLGA sample had 0.5 ml of the appropriate dihydrazide solution and 0.5 ml of the EDAC/NHS solution added to them, regardless of whether it was a PLGA coated coverslip, coated test-tube, or scaffold. These were allowed to react for two hours at room temperature with gentle shaking, and then the samples were rinsed three times with deionized water to remove the excess reactants. The next step was to either quantify the dihydrazides or to add the bone growth factors.
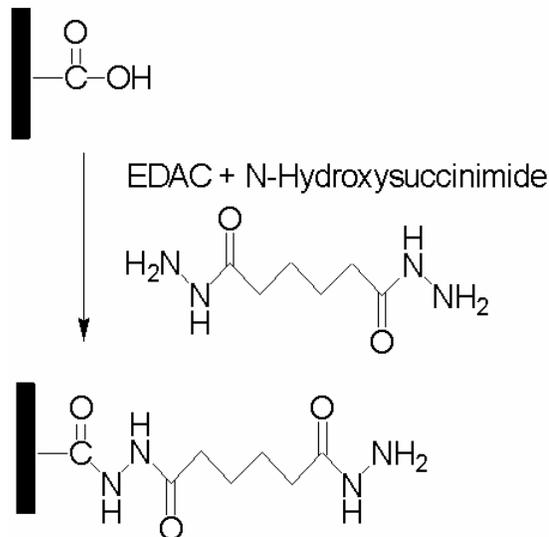
Figure 3.3.1b: Reaction scheme for the addition of dihydrazides to carboxyl groups

on the ends of the PLGA chain

3.3.1.1   Quantification of Dihydrazides with TNBS

Quantification of the dihydrazides on the PLGA was accomplished using a couple

of methods. The first method used a solution of 0.1% (w/v) 2,4,6,-trinitrobenzene

sulfonic acid (TNBS) (Sigma) in 3% sodium borate (Sigma). The TNBS solution (0.5

ml) was added to the rinsed PLGA-dihydrazide samples and heated at 70°C for 5 min,

causing a reaction where the free hydrazide group displaces the sulfonate group to form a

covalent bond with the remaining trinitrophenyl group. Next, 0.5 ml of 1 M NaOH was

added to the samples and heated for an additional 10 min to hydrolyze the trinitrophenyl

group. This hydrolysis step produced a yellowish-orange color that could be measured at

450 nm with a plate reader (Dynatech MR5000). The absorbance values of the samples

were then compared to those values produced from a standard curve produced with

known concentrations of dihydrazides to quantify the dihydrazides.

3.3.1.2 Quantification of dihydrazides with Alexa 350

Another method of quantification used was to react the hydrazides with the fluorophore Alexa 350 (Invitrogen). This method was only used for the PLGA coated test tubes and PLGA scaffolds. First, 5 mg of Alexa was dissolved in dimethyl sulfoxide (DMSO) (Sigma), giving a 8.123 mM stock Alexa solution. After aspirating the excess dihydrazides and rinsing the dihydrazide-treated PLGA samples with deionized water, 7 μl of Alexa 350 stock solution and 1.0 ml of PBS, pH 7.4, were added to each sample. The samples were then covered to keep light out and allowed to react for one hour. The excess Alexa was aspirated, and the remaining PLGA-dihydrazide-Alexa 350 component was dissolved in 1.0 ml of 100% acetone (Fisher). Fluorescence (excitation 346 nm, emission 443 nm) of the samples was then measured using a fluorometric plate reader (SpectraMax Gemini XS) with 0.1 ml of the dissolved Alexa- and dihydrazide-treated PLGA samples per well. These values were then compared to a standard curve constructed from the Alexa stock solution.

3.3.2 Heparin

A variety of methods were attempted to attach heparin (Sigma, ~13K MW) to the PLGA scaffolds directly and through the dihydrazide spacers. For detection of heparin, two methods of quantification were accomplished. These will be discussed in the sections that follow.

3.3.2.1 Oxidation of Heparin with Sodium Periodate

Sodium periodate (Sigma) was used to oxidize diols on the heparin chain to aldehydes. Briefly, 250 μl of 10 mM sodium periodate was added to 250 μl of a 40

µg/ml heparin stock solution. The sample was allowed to react in the dark for 45 minutes and then was quenched using 0.5 ml of a 10% glycerol solution. The sample was then filter centrifuged (Micron, Ultracel YM-3, 3000 MWCO) at 10,000g for 90 minutes to separate the oxidized heparin from the excess glycerol. Next, the filtered samples were rinsed with PBS, pH 7.4. The resulting oxidized heparin solution was diluted to 10 ml with deionized water and compared to a standard curve produced using the commercially available Blyscan assay (Biocolor, United Kingdom) to determine the yield of oxidized heparin.
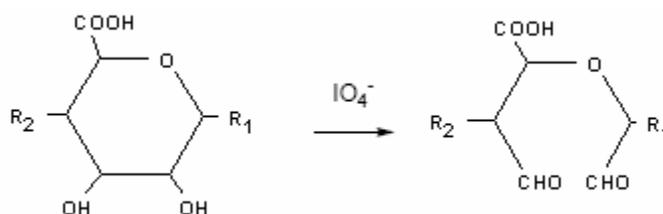
Figure 3.3.2.1: Reaction scheme for the oxidation of heparin diols to aldehydes

The procedure for using the Blyscan assay was as directed by the manual. Briefly, 100 µl of the sample was added to 1.0 ml of dye reagent and allowed to mix for 30 minutes. Next, the sample and dye reagent solution were centrifuged at 10,000g for 10 minutes, followed by removal of the supernatant liquid. Care was taken not to dislodge the bluish purple pellet. The Blyscan dissociation reagent (1.0 ml) was then added and vortexed to bring the pellet back into solution. The absorbance was measured at 656 nm and compared to a standard curve constructed using known quantities of heparin.

3.3.2.2 Heparin Addition with 1,1'-Carbonyldiimidazole

The method used to attach heparin directly to the PLGA scaffolds utilized 1,1'-carbonyldiimidazole (CDI) (Sigma) (Figure 3.3.2.2).[64] For this procedure, the scaffolds were soaked in 200-proof ethanol (Sigma) for 15 min using 0.5 to 1.0 ml of ethanol per scaffold. The ethanol was aspirated from the scaffolds followed by the addition of deionized water. Just enough deionized water was added to prevent the scaffolds from being completely submerged. Care was taken to note the volume added, then enough CDI was added slowly over a 15 min period to make a 0.2 M solution. The CDI solution was then aspirated from the scaffolds.
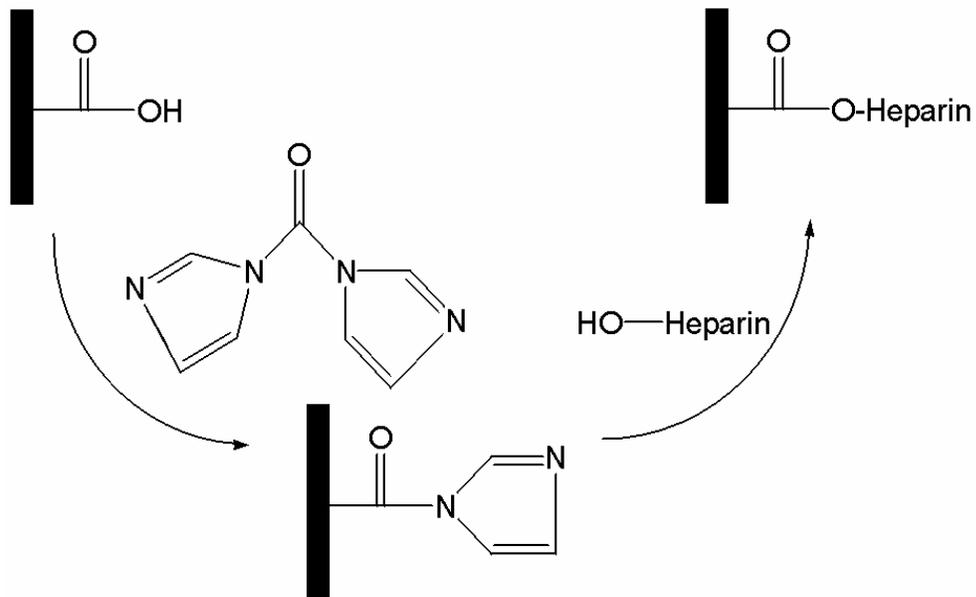
Figure 3.3.2.2: Reaction scheme for the addition of heparin to the carboxyl group on the ends of the PLGA chain

To compare heparin addition as a function of CDI treatment, excess heparin (0.5 ml of 1 mg/ml) was added to scaffolds treated with CDI and to scaffolds without CDI treatment, then both were diluted to 1.0 ml with 0.2% (w/v) NaCl solution. Blanks had only 1.0 ml of 0.2% (w/v) NaCl added to them. All scaffolds were then allowed to react

overnight on a rotator. The rotator was used to increase penetration of the heparin into the pores of the scaffold. After reacting overnight, the excess heparin was aspirated and the scaffolds were rinsed twice with deionized water.

3.3.2.3 Heparin Quantification

Heparin quantification on scaffolds involved the use of toluidine blue (t-blue) (Fisher Biotech) and the procedure referenced by Hermanson *et al.*[65] Here, 0.6 ml of 0.005% t-blue in 0.01 N hydrochloric acid containing 0.2% (w/v) NaCl and 0.4 ml of a separate 0.2% (w/v) NaCl solution were added to each scaffold after they were rinsed of excess heparin and allowed to react for 2 h on the rotator. After reacting for 2 h, the absorbance of the supernatant was measured at 631 nm using a Hitachi U-2000 spectrophotometer. These absorbance values were compared to a standard curve made with known heparin concentrations ranging from 6 µg/ml to 21 µg/ml. The Blyscan assay had a limited range and effectiveness with heparin attached to PLGA and was not used to quantify heparin attached to PLGA scaffolds.

3.3.3 Bone Morphogenetic Protein-2 Attachment

Human recombinant BMP-2 (1.0 mg) was obtained from Kamiya Biomedical Company in lyophilized form combined with an equal amount of human serum albumin (HSA). This was suspended in 0.5 ml of PBS, pH 7.4, and 0.5 ml of ultra-pure water then filtered using a SwellGel Blue Albumin Removal Kit (Pierce) per the manufacturer's instructions to remove the albumin. To determine the amount of BMP-2 available after using the albumin removal kit, a BCA assay (Pierce) was used as directed by the manufacturer's instructions.

Each heparin-loaded scaffold had 10 µg of BMP-2 added to it. This was slightly less than twice the mass of heparin that was attached to the scaffolds and yields a molar ratio of approximately 1:1 BMP-2 to immobilized heparin. PBS was added to make the final volume of BMP-2 solution 1.0 ml per scaffold. The scaffolds were allowed to react while on the rotator for 24 h. The excess BMP-2 solution was aspirated, and the scaffolds were rinsed twice with deionized water before the BMP-2 detection steps began.

3.3.3.1 Bone Morphogenetic Protein-2 Quantification

Detection of BMP-2 on the scaffolds was completed using a microBCA assay (Pierce). The instructions from the manufacturer were followed for construction of the standard curve and the mixing of the working reagent solution. Adaptation of the protocol for the detection of protein on the scaffolds involved the addition of 0.5 ml of the working reagent to each sample and incubation at 37°C with gentle shaking for two hours. After two hours, the absorbance of the samples was measured using a microplate reader (Dynatech MR5000) at 570 nm. These absorbance values were compared to a standard curve constructed using a stock bovine serum albumin (BSA) standard.

3.3.3.2 Bone Morphogenetic Protein-2 Orientation

Orientation of BMP-2 was probed using antibodies for the N- or C-terminus of BMP-2 (Santa Cruz Biotech; SC-6985 for N-terminal and SC-6267 for C-terminal antibodies). The procedure for attaching BMP-2 to the scaffolds was identical to the procedure mentioned in section 3.3.3. Scaffolds were blocked using 0.5 ml of 0.5% (w/v) BSA (Sigma-Aldrich) in 0.05% Tween 20 (Sigma) in PBS (PBST) after being

rinsed of excess BMP-2. This was allowed to react for 30 minutes on the rotator. Excess

BSA was rinsed off twice in 0.5 ml of PBST. The primary antibody, goat IgG against N-

or C-terminus of human BMP, was diluted 1:200 with PBS (90 μl in 18 ml of PBS) and

added at 0.5 ml per sample. Samples were allowed to react for 30 minutes at 37°C with

gentle shaking. The excess primary antibody was aspirated off, and the samples were

rinsed twice with PBST. The secondary antibody, anti-goat antibody conjugated to

alkaline phosphatase, developed in rabbit (Sigma), was diluted 1:8000 (3 μl in 24 ml) and

then added at 0.5 ml per scaffold. The samples were allowed to react for 45 minutes at

37°C with gentle shaking. Again, the excess was removed, and the samples were rinsed

twice with PBST. Finally, 0.5 ml of 0.1% (w/v) Sigma 104 phosphatase substrate

(Sigma) in 10% (v/v) diethanolamine (Curtin Matheson Scientific Inc, Houston, TX) was

added to each sample and allowed to react for 1 hour at 37°C. The absorbance of 100 μl

of each sample was then measured at 410 nm. The absorbance values were then used to

determine the effectiveness of the orientation procedure. This was done by comparing

the ratio of the absorbance values obtained to the mass of BMP-2 that was on the

scaffolds.

3.4   C3H10T1/2 Cells and Scaffold Bioactivity

C3H10T1/2 mouse pluripotent cells (CCL-226; ATCC, Rockville MD) were used

to assess the bioactivity of the BMP-2 loaded scaffolds. The first step in the process was

to load heparin and BMP-2 as directed above, but in a sterile environment. Four groups

of scaffolds were created to compare oriented BMP-2 attachment to random adsorption of

BMP-2 on the scaffolds (Table 3.4). Scaffolds that had adsorbed heparin (no CDI) with

BMP-2 loaded on them made up the first group. The second group was comprised of

scaffolds with BMP-2 that were without heparin and without CDI activation.   The third

group of scaffolds had covalently linked heparin with BMP-2. Scaffolds that were made

without heparin present, but were activated with CDI before the addition of BMP-2

comprised the fourth group. A fifth set of scaffolds that had no heparin and no BMP-2

treatment was also created. Once these five categories of scaffolds were prepared, they

were placed in individual wells of a 96 well plate and 250 µl of αMEM containing 1%

fetal bovine serum (FBS) medium (Invitrogen) containing 100,000 cells were added to

each well. In addition, a group of scaffolds without heparin or BMP-2 immobilized on

them were also placed in wells. These acellular scaffolds were placed in 250 µl of 1%

FBS medium. The scaffolds were then incubated at 37°C for three days. Following

incubation, the scaffolds were removed from the wells and placed in individual 2.0 ml

centrifuge tubes. They were then rinsed twice with PBS followed by the addition of 1.0

ml of high salt buffer (0.05 M NaH_2PO_4, 2 M NaCl, 2 mM EDTA, pH 7.4). The

scaffolds were then frozen at -70°C overnight and thawed the following morning. The

freeze-thaw cycle was repeated twice to ensure that the cells were lysed. Following the

final freeze-thaw cycle, the scaffolds were sonicated at 25 W to break up the scaffolds

and any remaining whole cells. Samples were then centrifuged at 4500g for 2 minutes to

separate the scaffold material from the cell material.

Table 3.4: Scaffold Treatment by Category for Bioactivity Determination

Group 1	Group 2	Group 3	Group 4	Group 5	Group 6
Hep+BMP	BMP	Hep+BMP	BMP	No Hep	No Hep
No CDI		CDI		No BMP	No BMP
C3H10T1/2 Cells					No Cells

A Hoechst DNA assay was then run on the samples to determine DNA content.

Briefly, 50 µl of a 0.5 µg/ml Hoechst 33258 solution was added to 200 µl of the

supernatant from above. The mixture was given a gentle shake before letting stand, covered from light, for 10 minutes. The fluorescence was then measured (356 nm excitation, 458 nm emission), and the values were recorded and compared to a standard curve constructed with known amounts of calf thymus DNA.

An alkaline phosphatase (AP) assay was also completed to determine the activity of the BMP-2 for each set of scaffolds. First, a substrate solution that was 10 mM Sigma 104 phosphatase substrate (Sigma), 0.6 M 2-amino-2-methyl-1-propanol buffer, and 4 mM $MgCl_2$ was prepared. This was then cooled to near freezing. Next, 50 µl of the substrate solution was added to 10 µl of the cell lysate and incubated at 37°C for 30 minutes. Absorbance was then measured at 410 nm. Activity was expressed as nmoles of substrate cleaved per minute (nmol/min) and normalized by total intracellular protein (nmol/min/µg DNA).

3.5   Statistical Analysis

Unless otherwise stated, the sample size was six for all experiments. All the graphs in the results section are displayed as the mean ± the standard deviation. Statistical analysis was performed using INSTAT3 software (Graphpad software, inc.). One way ANOVA was the primary method used to compare means from multiple groups for statistical significance. When appropriate, the Tukey Kramer multiple comparison test was used to compare the different experimental groups.

4   RESULTS

4.1   Microsphere Characterization using Particle Size Testing

     Particle size testing was accomplished on the microspheres produced with the use of the homogenizer as described in section 3.1.3 and on spheres that were produced when the magnetic stirrer was set to 450 rpm, also described in section 3.1.3. The results from testing the microspheres made using the homogenizer yielded a mean diameter of approximately 40 microns, which was too small for our use. The distribution of particle sizes for the spheres made with a magnetic stirrer at 450 rpm is shown in Figure 4.1.1. The median and mean particle diameters for those were 146 microns and 180 microns, respectively.
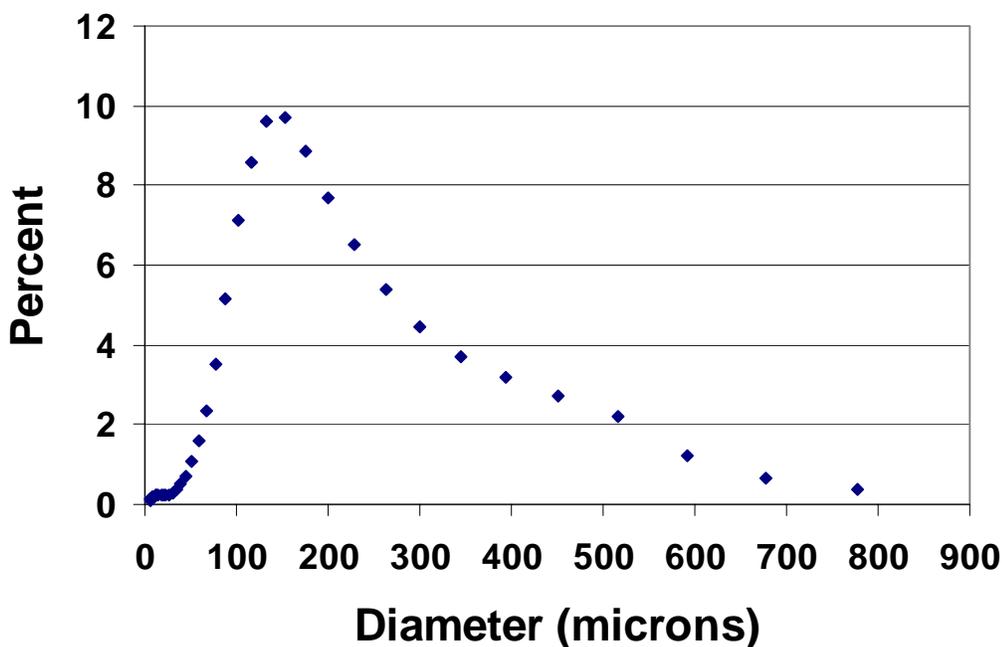
Figure 4.1.1: Particle size distribution for microspheres

4.2   Scaffold Characterization

4.2.1   General Scaffold Characterization

Pictures of the scaffolds are shown in the next two figures. The first picture (Figure 4.2.1a) shows a batch of scaffolds that were prepared by pouring microspheres greater than 150 μm in diameter into the mold and then heating at the T_g for 24 hours. The dimensions (approximately 4.8 mm diameter by 5.8 mm high) of the scaffolds can be seen in the second picture (Figure 4.2.1b). The scaffolds have a mass of approximately 55 mg and a density of 0.58 g/ml.

Figure 4.2.1a: Picture of PLGA scaffolds showing similar size and shape
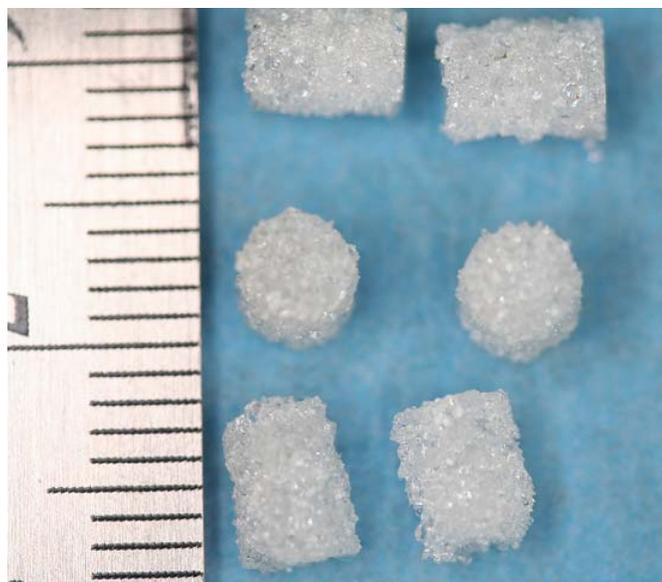
Figure 4.2.1b: Picture showing scaffold dimensions

4.2.2 Mercury Intrusion Porosimetry

Results from mercury intrusion porosimetry (MIP) testing of the initial 25 mg scaffolds made with 50-150 μm microspheres are shown in Table 4.2.2. The average porosity was 47.0% with a total pore area of 0.073 m^2/g per 15 scaffolds, resulting in an average surface area of 1633 mm^2 per scaffold.

Table 4.2.2: Mercury Intrusion Porisometry Data

Porosimeter data	units	Group 1	Group 2	Group 3	Average	std dev
total intrusion volume	mL/g	0.7729	0.7682	0.7215	**0.7542**	**0.0284**
total pore area	m^2/g	0.079	0.073	0.068	**0.073**	**0.0055**
median pore diameter(vol)	μm	38.3991	41.3219	41.8667	**40.5292**	**1.8648**
median pore diameter(area)	μm	29.0107	31.0564	32.8055	**30.9575**	**1.8993**
average pore diameter(4V/A)	μm	39.3351	42.0678	42.5957	**41.3329**	**1.7501**
bulk density at 0.21psia	g/mL	0.6144	0.6100	0.6466	**0.6237**	**0.0200**
apparent (skeletal density)	g/mL	1.1701	1.1481	1.2122	**1.1768**	**0.0326**
porosity	%	47.4896	46.8647	46.6545	**47.0029**	**0.4344**

4.2.3   Scanning Electron Microscopy

Scanning electron microscopy of scaffolds made with 50-150 µm microspheres revealed a structure that visually appeared more solid than porous when compared to scaffolds made with microspheres greater than 150 µm. An SEM image (Figure 4.2.3a) of the cross-section of a scaffold made with spheres < 150 µm in diameter shows that there were a few pores present with sizes greater than 100 µm. It was also observed that most of the microsphere sizes were smaller than the 50 µm minimum that was desired. Another SEM picture (Figure 4.2.3b) shows the surface of the scaffold made with the smaller diameter (<150 µm) microspheres. Again, there are pores present, but overall the scaffold appears more solid than it does porous.
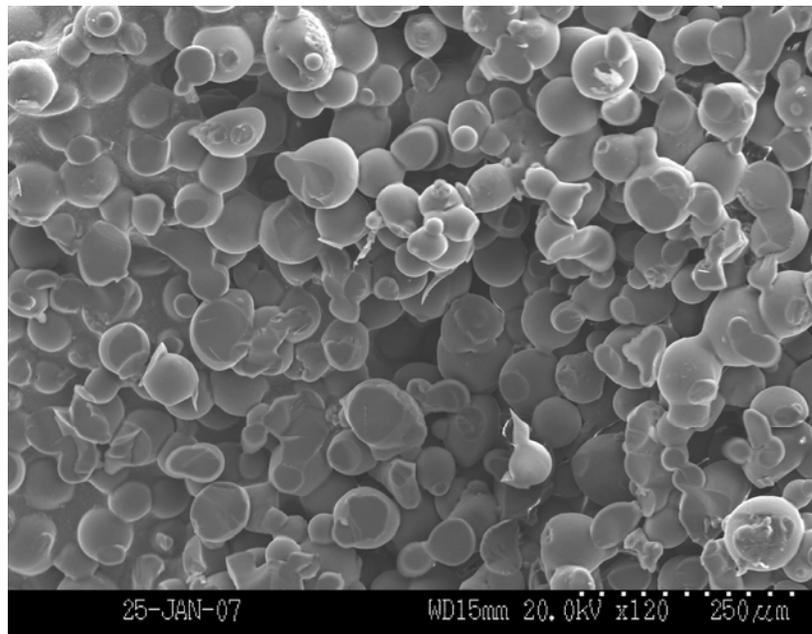
Figure 4.2.3a: Cross section of scaffold made with <150 µm diameter microspheres
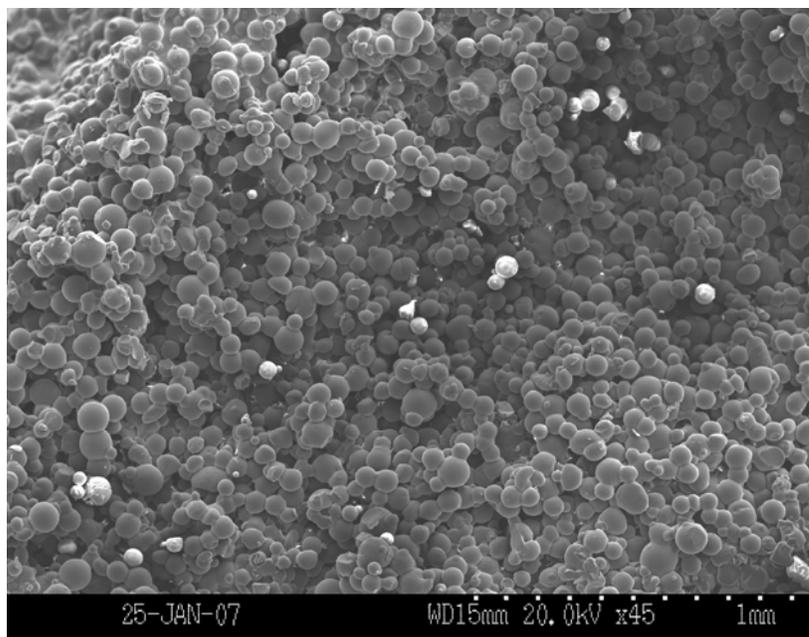
Figure 4.2.3b: Surface of scaffold made with <150 μm diameter microspheres

Scaffolds made with greater than 150 μm diameter microspheres showed much better porosity with some pore sizes over 200 μm in diameter based on SEM pictures. Figure 4.2.3c shows the cross-section of a scaffold made with the larger diameter microspheres and at a similar magnification as the cross-section of the scaffold made with smaller microspheres shown in Figure 4.2.3a. An SEM picture showing the surface view of a scaffold made with larger microspheres is shown in Figure 4.2.3d.

Another observation from the SEM pictures was that not all of the microspheres were greater than 150 μm as intended. Rather, there were aggregates of small diameter microspheres that had diameters greater than 150 μm. Nonetheless, there was still good porosity and good pore size with the larger diameter microspheres, especially when compared to the scaffolds made with smaller microspheres.
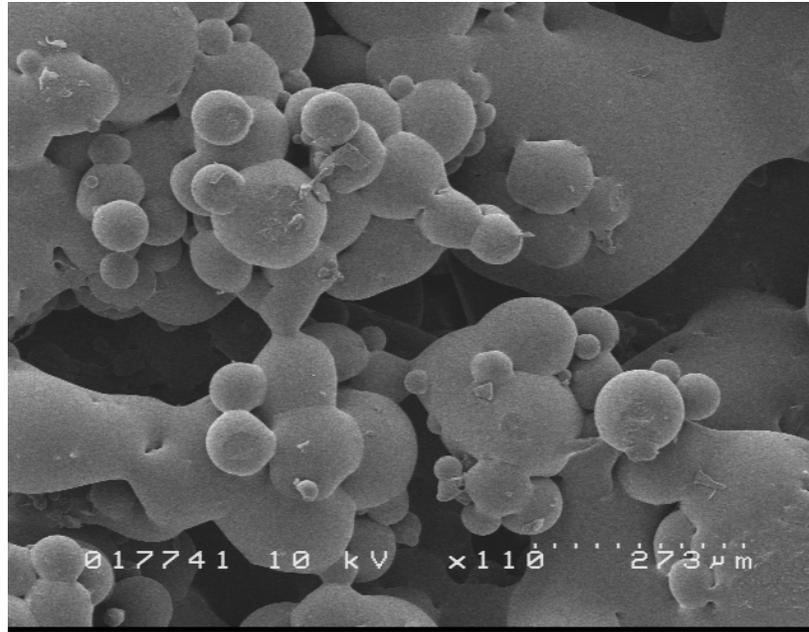
Figure 4.2.3c: Cross-section of scaffold made with >150 μm diameter microspheres
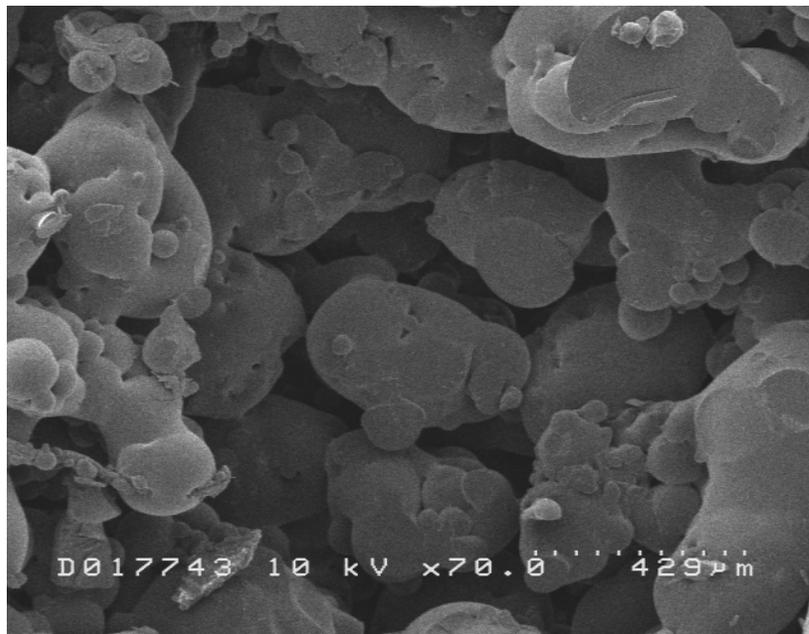
Figure 4.2.3d: Surface of scaffold made with >150 μm diameter microspheres

4.2.4　Mechanical testing

Results for compressive strength and modulus of the scaffolds tested are shown in

Table 4.2.4. These results were for scaffolds made with >150 μm diameter microspheres

and show an average compressive strength of 2.36 ± 0.23 MPa and an average modulus

of 30.1 ± 4.4 MPa. The production of scaffolds made with spheres <150 μm in diameter

had already been discontinued when the Bose mechanical tester had become available,

therefore there are no mechanical testing results for those scaffolds.

Table 4.2.4: Compressive Strength and Modulus of PLGA Scaffolds.

Scaffold	Strength (MPa)	Modulus (MPa)
1	2.17	38.9
2	2.43	28
3	2.26	29.5
4	2.54	27.1
5	2.07	27.9
6	2.66	29.4
avg =	2.355	30.13333
std dev =	0.22687	4.393935

4.3   Surface Modification

4.3.1   Dihydrazides

The four different dihydrazides used (see Figure 3.3.1 from Section 3) were

attached to PLGA using EDAC/NHS chemistry and were initially quantified using a

TNBS assay and later, using an Alexa fluorophore assay. The TNBS assay was used to

detect adipic dihydrazide (AAD) that was attached to PLGA-coated test tubes. Multiple

initial concentrations (0.018, 0.057, 0.115, and 0.184 mM) of AAD were used to

determine if it was possible to vary the amount of AAD on the surface by controlling the

initial concentration. The results (Figure 4.3.1a) in increasing numbers of molecules

from lowest concentration to highest concentration, were $1.73 \pm 2.3 \times 10^{15}$ molecules for

the lowest concentration to $3.4 \pm 7.97 \times 10^{15}$ molecules for the next, then to $4.59 \pm 2.65 \times$

10^{15} molecules for the third highest concentration, and finally to $5.22 \pm 4.0 \times 10^{15}$

41

molecules at the highest concentration of 0.184 mM AAD. The estimated surface area of polymer on the test tubes was 3.67 x 10^8 μm^2. Using that estimated area, the density of AAD molecules on the PLGA surface was determined and is also shown in Figure 4.3.1a. The surface densities ranged from 4.72 ± 6.24 x 10^6 molecules per μm^2 for the lowest initial concentration to 1.42 ± 1.1 x 10^7 molecules per μm^2 at the highest initial concentration. The trend on each of the graphs was as expected with higher initial concentrations having more molecules and a higher surface density than did the lower initial concentrations. The increase in the total number of molecules as the concentration increased was not linear however. For example, for a nearly three-fold increase in initial concentration of AAD from 0.018 to 0.057 mM there was a less than two-fold increase in the total number of AAD molecules retained and in the surface density for the same increase in concentration. Similarly, a nearly 10-fold increase from the lowest to the highest initial AAD concentration resulted in only a 3-fold increase in the AAD molecules retained and surface density. Statistical analysis using ANOVA indicated no significant difference between the mean values for each group.
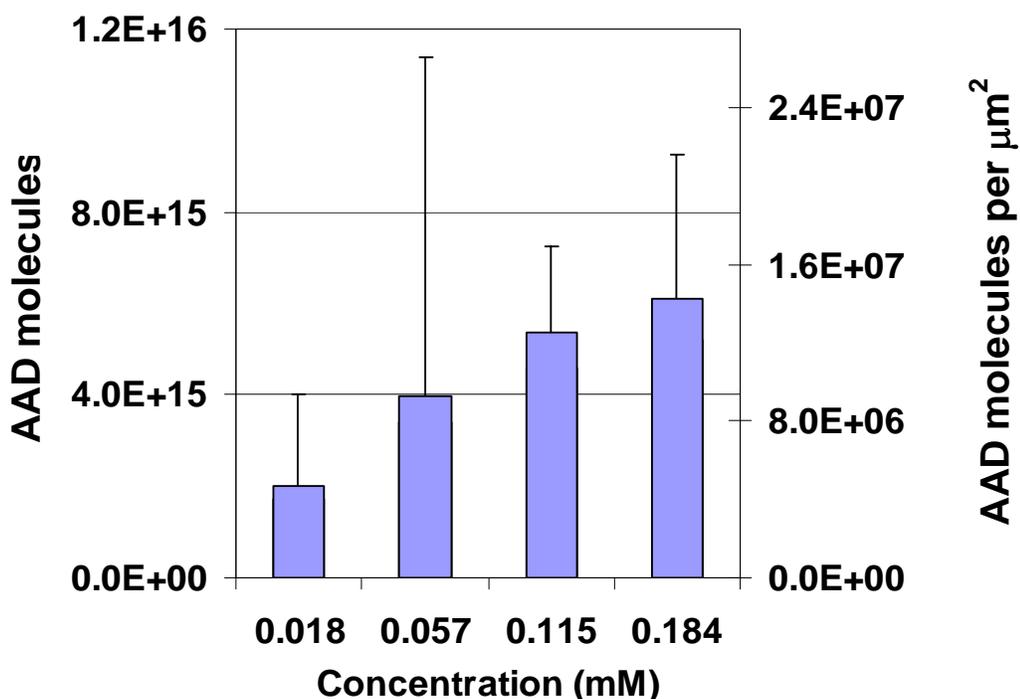
Figure 4.3.1a: Number and surface density of AAD molecules attached to PLGA-coated test tubes as a function of initial starting concentration

The first efforts to quantify dihydrazides using Alexa 350 were made using PLGA-coated test tubes to compare retention of dihydrazides on the PLGA when starting with equal molar amounts of each. The initial concentration was 131 mM for each dihydrazide and 0.5 ml (0.0656 mmol) were added to each PLGA-coated test tube. The results indicated that, given equal starting amounts in moles of the hydrazides, longer chain lengths led to more hydrazides being attached to the surface (See Figure 4.3.1b). ANOVA indicated that the molecules retained for the C10 dihydrazide group were significantly greater than the other groups ($p < 0.001$ for all three comparisons). There was no statistical difference between the C2, C4, and C6 dihydrazide groups.
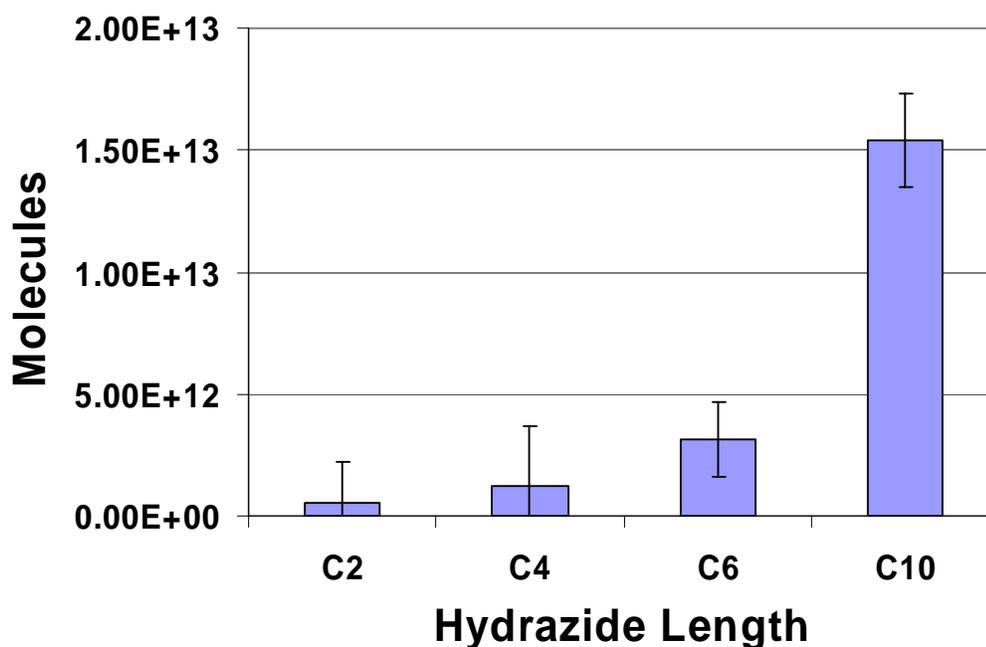
Figure 4.3.1b: Dihydrazides attached to PLGA-coated test tubes as a function of dihydrazide length

Another experiment was done using AAD and PLGA-coated test tubes, this time using Alexa 350 to determine the effect of different starting concentrations of the same dihydrazide on retention. This was similar to the experiment above that used TNBS to quantify the AAD. The results showed four times the number of AAD molecules remaining for a 10 and 100 fold increase in the initial amount of molecules (Figure 4.3.1c). The only significant difference, as determined by statistical analysis using ANOVA, was between the high and low starting concentrations ($p < 0.05$).
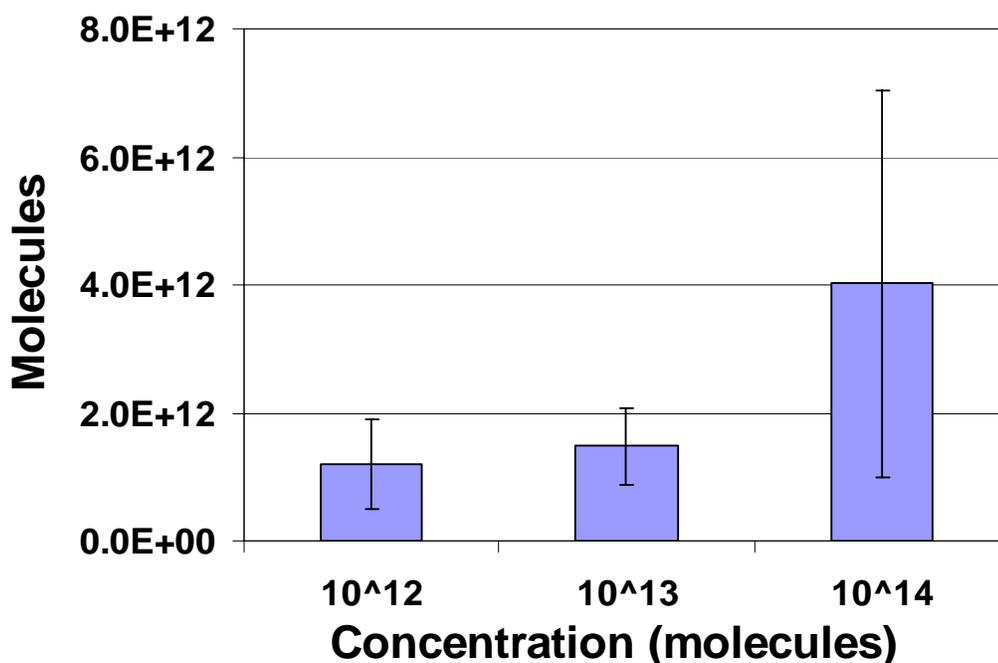
Figure 4.3.1c: AAD molecules attached to PLGA-coated test tubes as a function of initial starting concentration

4.3.2   Dihydrazides and Heparin

Early on, efforts were made to link oxidized heparin to the dihydrazides that were previously attached to the polymer surface. To determine the amount of oxidized heparin available after going through the oxidation process, the Blyscan assay was used. The results were an approximately 80% yield of oxidized heparin as compared to the initial mass.

However, the Blyscan assay was not effective at quantifying oxidized heparin that was attached to the dihydrazides on the PLGA coated test tubes. Efforts were made to attach oxidized heparin in a 1:1 molar ratio with the dihydrazides. Quantification of heparin immobilized in this manner was done using the Blyscan assay. However, the

results yielded no separation of absorbance values for samples that had oxidized heparin added to them compared with the absorbance values for blanks that were only PLGA. Further experiments determined that PLGA masked the Blyscan signal, preventing accurate detection of heparin attached to the polymer.

4.3.3 Heparin Alone

After the difficulties attaching oxidized heparin to the PLGA coated test tubes via the dihydrazides, it was decided to bypass using the dihydrazides and to link heparin directly with the polymer. To do this, 1,1'-carbonyldiimidazole (CDI) was used to create an ester linkage between the heparin hydroxyl groups and the free carboxyl groups on the ends of the PLGA chains. Experiments were designed to compare covalent heparin attachment using CDI with randomly adsorbed heparin on the surface of the PLGA scaffold.

Multiple sets of data need to be compared with regards to heparin attachment beyond the comparison of covalent attachment with CDI and random adsorption without CDI. When this experiment was initially conducted, the PLGA molecular weight was approximately 17 kDa (based on the viscosity data supplied with the PLGA source) and less than 150 μm diameter microspheres were used to make the scaffolds. Subsequently, it was decided to make the scaffolds using microspheres that were greater than 150 μm in diameter. Another variable was introduced when the original PLGA supply was exhausted. The new PLGA had a molecular weight (9.3 kDa) nearly half that of the original polymer used. Therefore, scaffolds made with 17 kDa PLGA and microsphere sizes greater than 150 μm were compared to scaffolds from the same molecular weight PLGA made with less than 150 μm spheres (Figure 4.3.3a). In this scenario, scaffolds

made with large microspheres that used CDI to covalently attach heparin had 16.03 ±

8.48 μg of heparin attached compared to only 3.45 ± 2.01 μg of adsorbed heparin on

scaffolds made with the same larger microspheres (p < 0.01). In contrast, scaffolds made

with 17 kDa PLGA and less than 150 μm microspheres had 8.06 ± 2.02 μg for covalently

attached PLGA and 2.6 ± 2.3 μg for adsorbed heparin. This difference was not

statistically different.
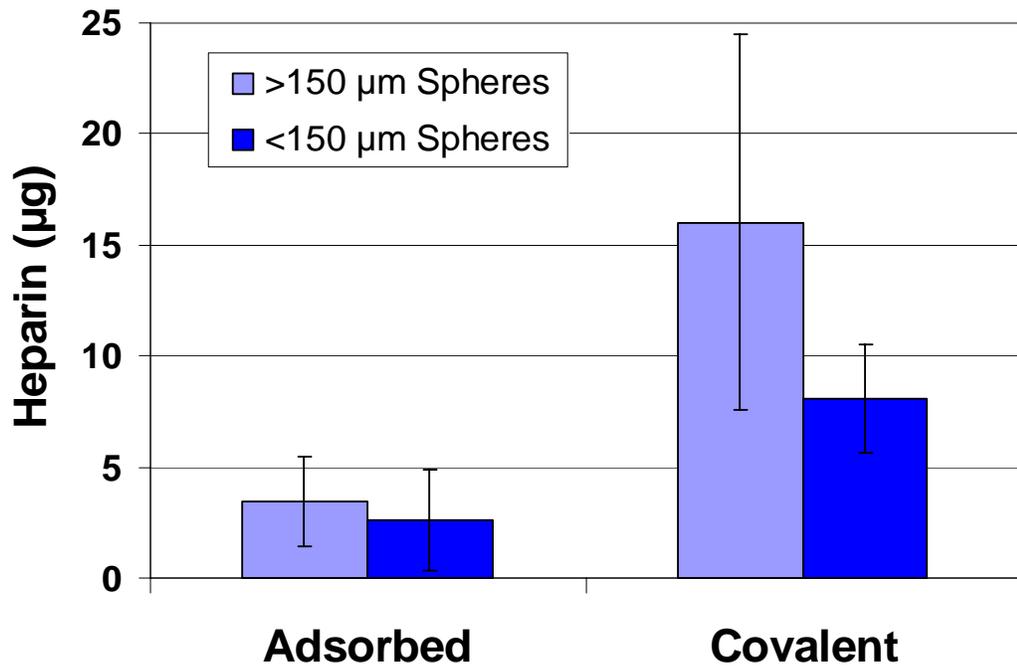
Figure 4.3.3a: Amount of heparin on scaffolds made with 17 kDa PLGA as a

function of heparin attachment type and microsphere size

Heparin loading experiments were also conducted on scaffolds made with the

lower MW PLGA that was obtained after all the 17 kDa PLGA had been consumed. All

of these scaffolds were made with microspheres greater than 150 μm in diameter. The

mass of heparin attached to scaffolds made with this MW PLGA was 6.64 ± 3.53 μg for

covalently attached heparin using CDI and 4.73 ± 1.77 μg for adsorbed heparin (Figure

4.3.3b) However, a t-test performed on the two groups indicated that the difference was not statistically significant.
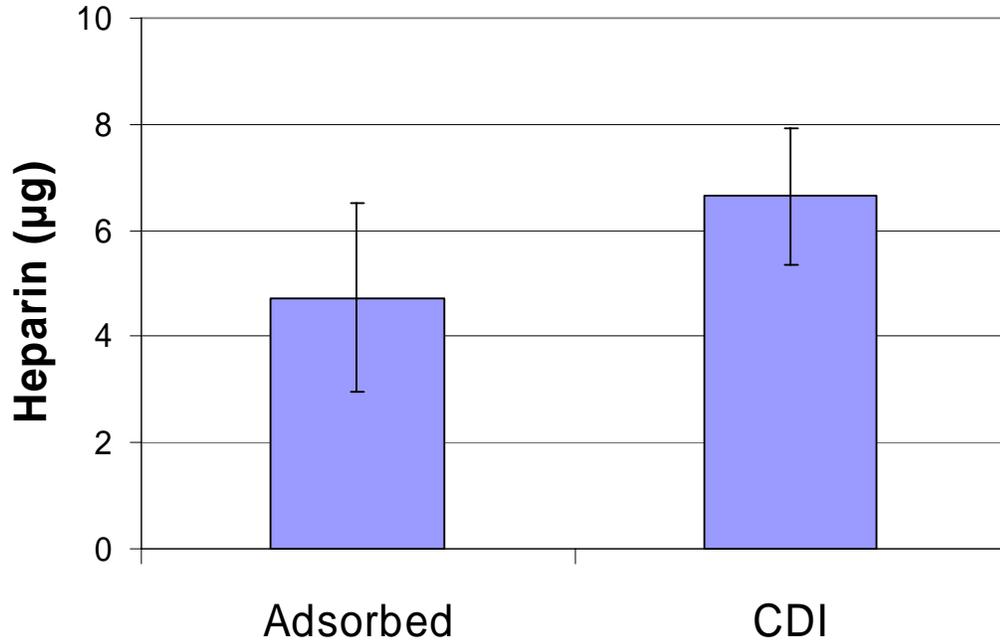
Figure 4.3.3b: Amount of heparin on scaffolds made with 9.3 kDa PLGA as a function of heparin attachment type

4.4 BMP-2 Attachment

Results from BMP-2 attachment are shown in Figure 4.4. Scaffolds with heparin covalently attached had more BMP-2 linked (1.23 ± 0.53 µg) than either scaffolds that had CDI treatment without heparin addition (0.767 ± 0.30 µg) or scaffolds that had BMP-2 linked to adsorbed (no CDI treatment) heparin (0.468 ± 0.14 µg). The mass of BMP-2 adsorbed to the surface of the scaffolds was 0.443 ± 0.15 µg. Statistical analysis using ANOVA revealed that differences between BMP-2 immobilized with the covalently linked heparin was significantly different than either the BMP-2 loaded on scaffolds with adsorbed heparin ($p < 0.01$) or the BMP-2 that adsorbed to the scaffold surface without

heparin ($p < 0.01$). The difference was not significant when compared to BMP-2 that was immobilized on scaffolds that had CDI treatment, but did not have attached heparin.
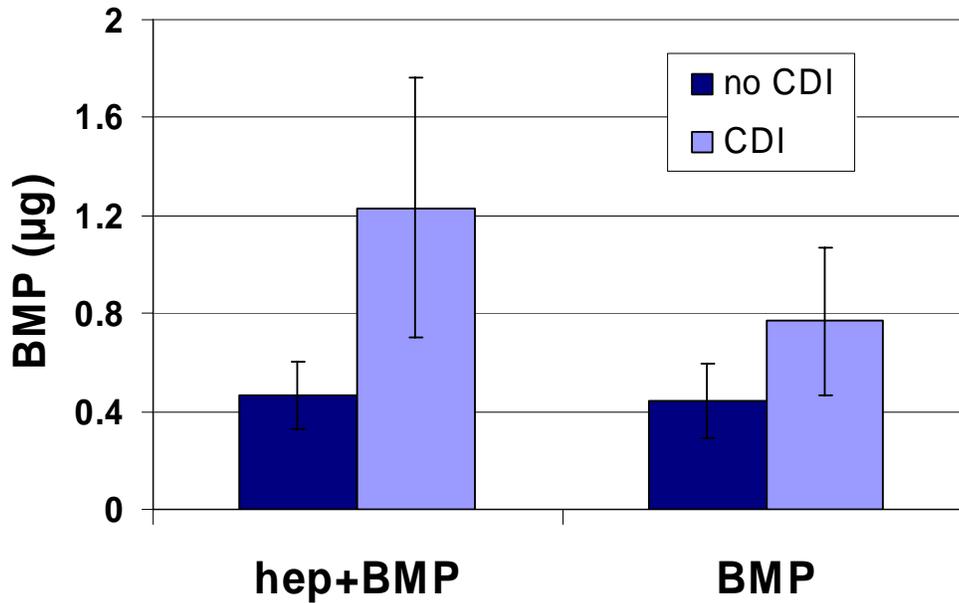
Figure 4.4: Amount of BMP-2 immobilized on PLGA scaffolds as a function of heparin loading type and/or CDI treatment

4.5   BMP-2 Orientation

The absorbance values for the N- and C- terminus antibody tests are shown in Figures 4.5a and 4.5b. The ratios of the absorbance values for the N- and C- terminus antibody test to the mass of BMP-2 on the different scaffold categories are shown in Table 4.4. The absorbance values and their ratios to the mass of BMP-2 immobilized were used to determine the effectiveness of immobilized heparin at orienting BMP-2 on the PLGA scaffolds. These results were not conclusive with regards to determining whether the BMP-2 was immobilized in the desired orientation. None of the differences

were statistically significant. However, the results did confirm the presence of BMP-2 on the scaffolds.
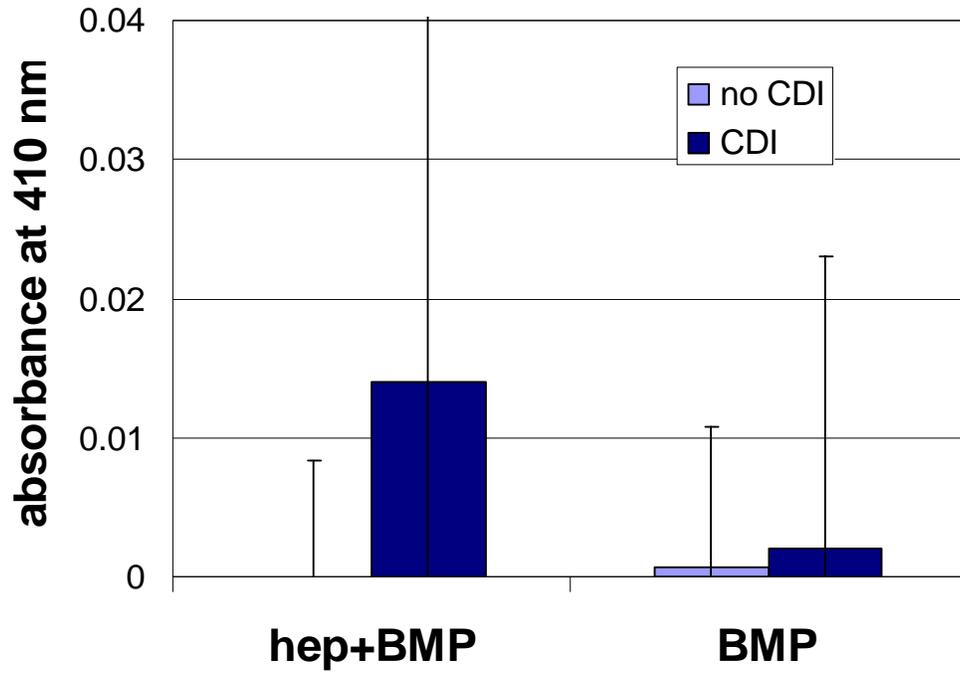
Figure 4.5a: N-terminal antibody test on BMP-2 loaded scaffolds
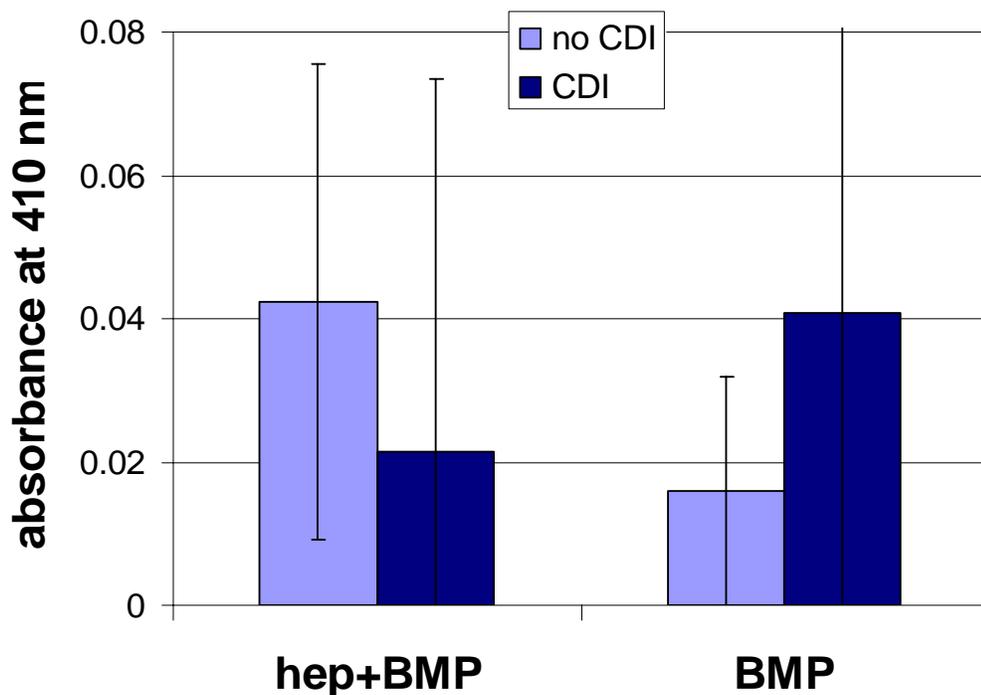
Figure 4.5b: C-terminal antibody test on BMP-2 loaded scaffolds

Table 4.5: Ratios of Absorbance to BMP-2 Mass on PLGA Scaffolds

	No CDI		CDI	
	Hep+BMP	BMP	Hep+BMP	BMP
N-terminus	0.000	0.002	0.011	0.003
C-terminus	0.091	0.036	0.017	0.053

4.6   C3H10T1/2 Cells and Scaffold Bioactivity

The DNA and AP assay results are listed in Table 4.6 and shown in Figure 4.6a

and 4.6b. Results of the DNA assay indicated that there was almost twice as much

cellular growth on the scaffolds that did not use CDI (groups 1 & 2) to activate the PLGA

carboxyl groups compared to the scaffolds that did use CDI (groups 3 & 4). The

scaffolds without BMP-2 immobilization (group 5) also had more cell growth than did

the CDI activated scaffolds with BMP-2 immobilization.

Table 4.6: Responses of C3H10T1/2 Cells to Scaffolds with Immobilized BMP-2

	Group 1	Group 2	Group 3	Group 4	Group 5
	Hep+BMP	BMP	Hep+BMP	BMP	No Hep
	No CDI		CDI		No BMP
	C3H10T1/2 Cells				
DNA (µg)	0.156±0.040	0.147±0.027	0.076±0.032	0.060±0.022	0.113±0.029
AP Activity (nmol/min/µg DNA)	7.51±2.08	5.99±0.34	18.95±2.56	18.39±7.47	9.62±2.58
AP Activity Normalized (per µg BMP-2)	16.05	13.52	15.41	23.98	

The AP activity assay results indicated that the oriented immobilization of BMP-2 using covalently attached heparin (group 3) stimulated significantly greater activity than both scaffolds that had BMP-2 simply adsorbed without heparin or CDI activation (group 2) ($p<0.001$) and scaffolds that used adsorbed heparin to immobilize BMP-2 (group 1) ($p<0.001$). The results also indicated no significant difference in activity between scaffolds that had been activated with CDI, regardless of the presence of heparin (groups 3 & 4). However, there was nearly 50% error associated with scaffolds that had BMP-2 randomly immobilized directly to scaffolds with CDI activation and no heparin present (group 4) compared to only approximately 13% error with scaffolds that used covalently attached heparin to immobilize the BMP-2 (group 3). Scaffolds without either BMP-2 or heparin (group 5) present had greater activity than did both sets of scaffolds from groups 1 and 2, although this difference was not statistically significant. The difference in activity between those scaffolds without BMP-2 or heparin present and the scaffolds that had CDI activation was statistically significant though ($p<0.01$ in both cases).
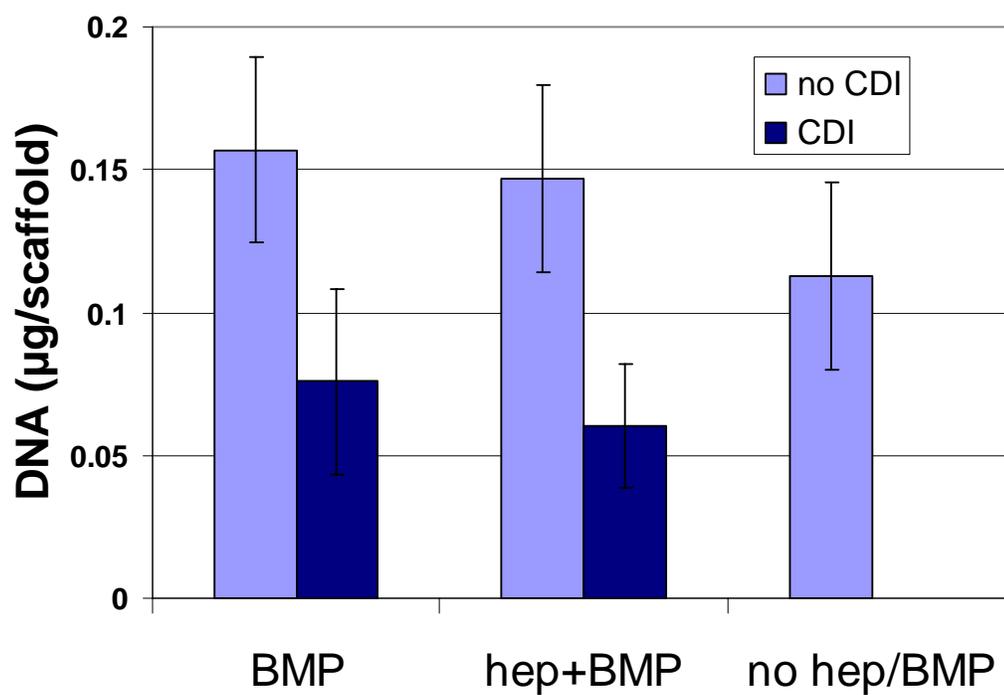
Figure 4.6a: DNA content as a function of BMP-2 immobilization method
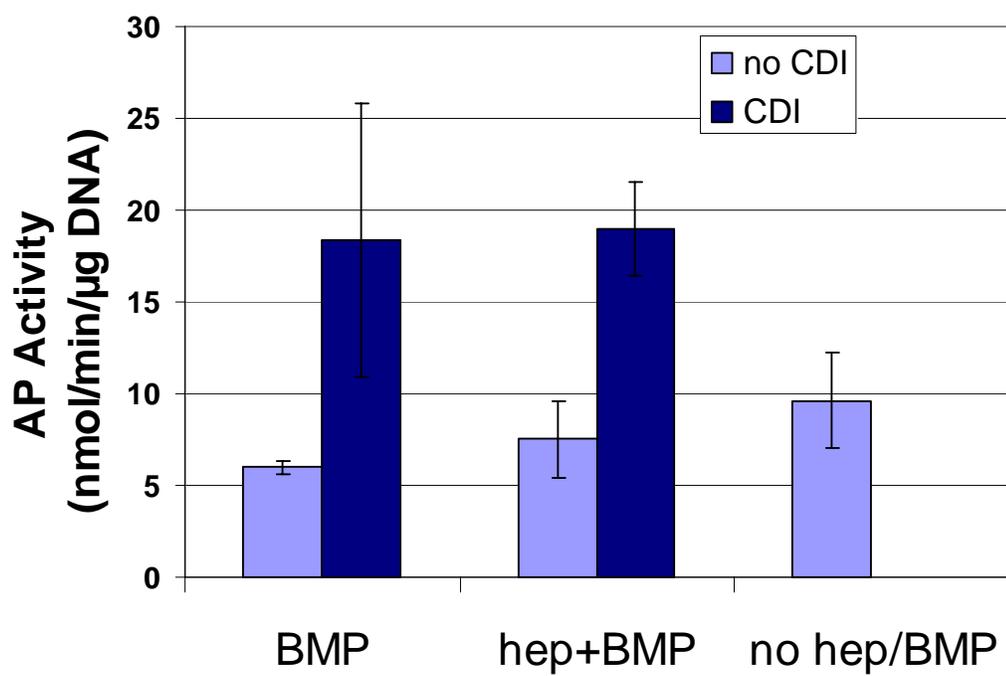
Figure 4.6b: AP activity as a function of BMP-2 immobilization method

5   DISCUSSION

5.1   Microsphere Characterization using Particle Size Testing

After results indicated that scaffolds made with larger diameter microspheres retained more heparin, particle size testing was done to determine the range of diameters produced for microspheres prepared using the homogenizer and for microspheres made with the magnetic stirrer at 450 rpm. Microspheres that were prepared using the magnetic stirrer at 600 rpm did not undergo particle size testing because SEM pictures revealed that those microspheres were too small to be effective. The method using the homogenizer to prepare microspheres resulted in diameters that were too small to make scaffolds with effective pore sizes (greater than 100 μm). Therefore, the use of the homogenizer was discontinued. Reducing the rotation speed of the magnetic stirrer to 450 rpm instead of 600 rpm resulted in microsphere diameters approximately 100 microns larger than the spheres produced with the homogenizer.

Borden, *et al.* used PLGA with an 85/15 ratio and a molecular weight (MW) of 420 kDa to make microspheres that were used for porous PLGA construction in one experiment. In another experiment, the same group used 50/50 PLGA with a MW of 50 kDa, a 75/25 ratio with MW of 92 kDa, and 85/15 ratios with 420 kDa and 92 kDa to make microspheres for use in scaffold preparation.[2, 7] They were able to produce scaffolds made with microspheres that had diameters of 600-710 μm, 355-425 μm, and 212-250 μm for the 85/15 & 420 KDa PLGA. The microsphere sizes were all between 425 and 610 μm for the second experiment they conducted. This was in contrast to the scaffolds made with our microspheres that had diameters of just over 150 μm. For this thesis research, there were not enough microspheres larger than 150 μm in diameter to

make enough scaffolds to be useful for experimental purposes. This suggests that higher

molecular weight PLGA chains with a greater ratio of lactic acid to glycolic acid could be

more appropriate for producing larger microspheres. For the current work, reducing the

spinning speed from 600 rpm to 450 rpm partially compensated for the low molecular

weight PLGA that was used.

5.2 Scaffold Characterization

5.2.1 General Scaffold Characterization

The pictures of the scaffolds in Figures 4.2.1 showed that all the scaffolds

produced were generally the same size and shape. They were not identical though and

certainly some of the error in the results was due to the variations in size from scaffold to

scaffold. For instance, smaller scaffolds had less surface area available for spacer and

growth factor attachment than larger scaffolds. Even a small difference in surface area

led to a much larger difference at the molecular level with respect to biomolecule

attachment, and accounted for some of the variations seen in the results.

5.2.2 Mercury Intrusion Porisometry

The MIP data for the scaffolds made using 25 mg of 50-150 μm diameter

scaffolds indicated an overall porosity that was less than that of cancellous or trabecular

bone (47% versus approximately 70%).[7] The mean pore diameter, depending upon the

calculation method (Micrometrics software), was between 30 and 41 μm. It is generally

agreed upon that for adequate penetration of cells and the resulting acceptable integration

of the material with the host tissue, the pore diameter should be at least 100 μm in

diameter.[7] The mean diameter of pores in these scaffolds were on the low end of the

trabecular bone porosity range and were well below the typical pore diameter that is considered suitable for supporting cell growth. However, based on MIP data and SEM images there were pore sizes that were much larger than the mean diameter and therefore in agreement with the generally accepted 100 μm diameter minimum diameter for cell and tissue penetration. Also, our objective was not to make scaffolds that completely mimicked trabecular bone and there are results that will be discussed below that suggest scaffolds with lower porosity than trabecular bone may be acceptable for integration of the material into the native bone tissue. Nonetheless, it was decided to use the greater than 150 μm diameter microspheres for scaffold fabrication based on the MIP data combined with the information obtained from the SEM images.

MIP data was not available for the scaffolds made with the larger spheres. However, it was expected that MIP data would show significantly higher porosity and larger mean and median pores sizes when compared to scaffolds made with microspheres less than 150 μm in diameter. This assumption was based on SEM comparisons between scaffolds made with small diameter microspheres and scaffolds made with large diameter microspheres.

Borden, *et al.* fabricated scaffolds with 600-710 μm diameters using the sintered microsphere approach that had median pore sizes of 210 μm and 35% porosity. Although their scaffold porosity was low in comparison to trabecular bone, their results showed acceptable penetration of cells into the scaffolds. Other groups that used the gas-foaming/salt-leaching or solution-casting/salt-leaching methods produced scaffolds with average pore sizes of approximately 50-200 μm and > 85 % porosity.[18-20, 66] The studies that looked at cell growth and proliferation reported positive results with those

pore sizes and porosity.[18-20] This suggests that scaffold porosity might not be the deciding factor when predicting the success of cellular proliferation on and in a biomaterial. It also further supports the use of PLGA as an effective material for eliciting a desired cellular response.

5.2.3   Scaffold Characterization Using SEM

Figures 4.2.3a and 4.2.3c both show the cross-sections of scaffolds at a similar magnification. The scaffolds made with larger diameter microspheres (Figure 4.2.3c) showed greater porosity with many pores being well over 200 μm in diameter when compared to the scaffolds made with the smaller microspheres that had only a few pores with diameters over 100μm (Figure 4.2.3a). Results from the previously mentioned studies where porosity was greater than 85% and the pore sizes were in the 100-200 μm range suggest that the scaffolds made with larger diameter microspheres would be more appropriate for supporting cell growth.[18-20] This information provided further support for abandoning the fabrication of scaffolds made with less than 150 μm diameter microspheres.

SEM images of the surface of scaffolds are shown in Figures 4.2.3b and 4.2.3d. These pictures, illustrate that there was little porosity on the scaffolds made with smaller microspheres (Figure 4.2.3b) and that the larger microsphere scaffolds have larger pore sizes and increased porosity (Figure 4.2.3d). The SEM image of the cross-section of the large microsphere scaffolds also suggests that adequate porosity exists throughout the scaffold, further supporting the premise that these scaffolds would be well suited for cell infiltration.

It is important to note that in the scaffolds made with the larger sphere size, not all the microspheres were greater than 150 μm in diameter. In some cases there appeared to be aggregates of small microspheres that were greater than 150 μm in diameter. It was likely that these aggregates formed before the sieving process since the smaller microspheres would be removed at that time. That means they could have formed either during the lyophilization process or during the drying process that occured when the microspheres were being recovered but before they were placed in the -70°C freezer. Regardless of the formation of these aggregates, characterization of the scaffolds made with >150 μm diameter microspheres (or in some cases, aggregates that are >150 μm in diameter) indicated they were well suited for integration with the host bone tissue. Additional studies are needed to examine the effects of reducing the formation of the aggregates and increasing the yield of larger microspheres.

5.2.4 Mechanical Testing

While reports vary somewhat, the compressive strength of cortical and cancellous bone is typically 120-150 MPa and 10-50 MPa, respectively.[67, 68] Reports for Young's modulus of cortical and cancellous bone also vary somewhat, but are near 15-30 GPa for cortical bone and between 0.5-1.0 GPa for cancellous bone.[8, 67, 68] Results from mechanical testing done on the PLGA scaffolds fabricated in this experiment indicated they would be weak when compared to both cortical and cancellous bone. However, these scaffolds were not designed to replace the natural bone, rather they were made to fill the defect site, and then degrade as they induced new bone formation into that site. To do this, the scaffolds need to be osteoinductive and able to provide structural support for cell attachment and growth.

One study that fabricated scaffolds for cell growth determined that their scaffolds had a compressive strength of approximately 0.2 MPa with a modulus at ~ 3.9 MPa.[18] These scaffolds had a porosity of about 90%, were manufactured using a particulate leaching method, and were shown to support fibroblast cell growth. Another study that fabricated scaffolds using the sintered microsphere approach reported a compressive modulus of 232 MPa for scaffolds with 35% porosity.[7] This study also reported osteoblast growth on and into their scaffolds.

Comparing the mechanical properties of the two previously mentioned studies to those reported in the results section (Table 4.2.4) suggests that our scaffolds are mechanically adequate and able to support cell growth. However, as mentioned before the primary purpose of the scaffolds designed for this project was to fill the defect site and then to induce the formation of native bone tissue into that site.

5.3   Spacer Immobilization

All the surface modifications were made with the purpose of improving the bone regeneration capacity of the PLGA scaffolds. The initial efforts made in the surface modification process involved the attachment of spacers, either hydrazides or heparin, then the quantification of those spacers. These spacers were then used as the attachment points for the BMP-2 that was immobilized.

Quantification of the spacer molecules was difficult, regardless of whether the spacer was a dihydrazide or heparin. The reasons will be discussed below, but the problems with quantification also made determining the optimal surface density of spacers and optimal spacer length even more difficult to accomplish.

5.3.1   Dihydrazide Immobilizaton

The first efforts to quantify spacers, given the same dihydrazide type (AAD) and different initial concentration, were made on PLGA coated glass test tubes using TNBS as the method for detection and quantification. The purpose of this particular experiment was to determine how effective it would be to control the surface density of the dihydrazides by measuring the total amount of hydrazide molecules retained and by determining the amount of molecules per unit surface area. The results suggested that higher initial starting amounts of AAD do result in more AAD retained on the surface. However, the results were not statistically significant.

There are a couple of potential reasons for the differences not being statistically significant. First, the TNBS assay was deemed to lack the sensitivity to give a reliable count of the hydrazide molecules at that low of a concentration. The absorbance values obtained for the samples were typically on the low end of the TNBS standard curve. Also, this portion of the TNBS standard curve was associated with the highest degree of uncertainty which was likely due to the small numbers of molecules at the low end of the curve ($\sim 10^{15}$) and the corresponding inconsistent absorbance values obtained using TNBS for those numbers of molecules.

Another potential source of the large error range was the PLGA surface itself. It was difficult to consistently reproduce the exact surface area regardless of whether it was PLGA-coated test tubes or PLGA scaffolds. Also, the number of dihydrazide molecules that were attached was a function of the amount of carboxyl groups from the PLGA chains that were available in a given area. Assuming that the height of the PLGA in the test tubes was 4.0 ± 0.25 mm, there could be a difference of 18 million μm^2 in surface

area from test tube to test tube. It is possible that this potential difference in surface area could lead to a large difference in the amount of carboxyl groups between different test tubes. The differences in the surface area from test tube to test tube likely accounted for the majority of the uncertainty and the statistical insignificance associated with the results.

Efforts were also made to determine dihydrazide retention on the PLGA-coated test tubes as a function of the dihydrazide type. Alexa 350 was used to quantify the dihydrazides, because of the concern for the sensitivity of the TNBS. The results indicated that the largest dihydrazide, the C10 or sebacic dihydrazide, had superior retention in comparison to the smaller dihydrazides given the same initial starting concentration. One possibility for the results indicating increased retention with the C10 dihydrazide may be related to steric hinderance. There may have been enough steric hindrance from the surrounding polymer on the smaller dihydrazides to cause interference with the binding of Alexa 350 to the free hydrazide portion of the immobilized dihydrazides. Therefore, if the smaller dihydrazides bound in the same percentages as the C10 dihydrazide, they may not have been detected because the free hydrazide end was hindered from binding with the Alexa 350 in solution. Another possibility was that the longer length of the C10 dihydrazides may have led to a more favorable alignment of the free hydrazide functional groups for binding with the Alexa.

Because TNBS was initially used to quantify AAD for the surface density experiment, a similar experiment was designed where Alexa 350 was used to quantify AAD retention on PLGA coated test tubes. This time the initial starting concentrations were less than before (10^{14}, 10^{13}, and 10^{12} versus $\sim 10^{20}$ molecules). The main reason for

decreasing the initial starting concentration was that there was a very large excess of dihydrazide molecules when compared to what could theoretically be expected to be in a given area with the initial concentrations where they were. It was also convenient for comparison purposes to have 10-fold increases in the amount of initial starting concentrations of molecules. The results with this test also implied that higher initial starting concentrations led to more molecules retained, which further indicates that controlling the surface density of spacer molecules on the biomaterial surface is feasible. However, the only statistically significant difference was between the starting concentrations containing 10^{14} and 10^{12} molecules. Again, this was due to the large standard deviations, which were likely due to the variations in the PLGA surface area.

5.3.2 Dihydrazides and Heparin

Numerous studies have shown that heparin has a strong affinity for BMP-2 and generally improves the bioactivity.[15, 35, 45, 61, 69] Using this knowledge, efforts were made to link heparin with dihydrazides that were immobilized on the PLGA surface. This was done by oxidizing the diols on heparin to aldehydes so that they would react with the hydrazide functional groups to create a hydrazone linkage. The Blyscan assay was used to quantify the heparin that was immobilized in this manner, however it was not successful because the PLGA masked the signal that the heparin would have produced. The method that uses toluidine blue to detect heparin was not used to detect heparin bound to the immobilized dihydrazides on the biomaterial surface. This was primarily because it was determined that it would be more efficient to attach heparin directly to the PLGA surface.

5.3.3 Heparin

Results from the direct attachment of heparin to the PLGA scaffolds without the use of dihydrazides confirmed that the dihydrazides were not actually needed for heparin attachment. The main purpose of this experiment was to confirm that the use of CDI to covalently attach heparin to the scaffolds would result in more heparin immobilized on the surface than would random adsorption of heparin.

The results also indicated that scaffolds made with larger microspheres (>150 μm in diameter), given the same molecular weight of PLGA and the same initial concentration of heparin, retained more heparin on the surface than did scaffolds made with smaller microspheres. The rationale for this was that the scaffolds made with larger microspheres conceivably had more surface area than did the small microsphere scaffolds. These results combined with the pore sizes and porosity associated with the scaffolds made with larger microspheres further supported the premise that scaffolds made with the larger microspheres had greater potential to be used as a tissue engineering tool for inducing bone regeneration.

One other notable observation from the results was that scaffolds made with higher molecular weight PLGA showed better heparin retention than did scaffolds made with smaller molecular weight when both were made with greater than 150 μm microspheres. The suspected reason for this was that the larger molecular weight PLGA would more readily form larger microspheres and therefore produce more microspheres with larger mean diameters. Larger diameter microspheres would lead to scaffolds with increased surface area which could result in more biomolecules attached to the biomaterials surface. There is some support for this theory based on the results by

Borden, *et al*.[2, 6, 7] They used a variety of PLGA with different ratios of PGA to PLA with molecular weights ranging from 50 kDa to 420 kDa to conduct their experiments. In comparison, the PLGA used for this thesis was approximately 9-23 kDa. Their results showed the formation of microspheres with diameters ranging from 212 μm to 710 μm and the ability for osteoblast penetration into their scaffolds. The objective of this thesis did not involve the examination of osteoblast penetration, so a direct comparison cannot be made. However, they achieve larger diameter microspheres using larger MW PLGA.

Other studies have looked at the ability of heparin to enhance the effects of BMP-2 on different cell types. Experiments by Kamijo, *et al*. showed that heparin enhanced the effect of BMP-2 on C2C12 myoblasts *in vitro* and *in vivo*.[35, 45] However, these studies used heparin in solution at concentrations up to 30 μg/ml, instead of binding it to the surface of the biomaterial.

In other studies heparin was immobilized onto porous PLGA microspheres and to PLGA scaffolds.[16, 17] Amino-terminated PLGA was used to get 95.8 pmole (1.15 μg) of heparin/mg of microspheres.[16] Assuming a microgram of microspheres was equivalent to a microgram of scaffolds; this would have resulted in 63 μg of heparin per scaffold at a mass of 55 mg per PLGA scaffold. However, when using the same amino-terminated PLGA to make scaffolds (10 mm diameter by 2 mm thickness, but no indication of the mass of scaffolds or of the porosity), only 36.9 pmole (0.443 μg) of heparin per scaffold was able to be immobilized.[17] This was less than 0.3% of the heparin initially loaded onto the scaffolds. In comparison, using carboxyl-terminated PLGA scaffolds (from this thesis experiment) with CDI to immobilize heparin on the PLGA surface resulted in 3.2% of the initial heparin amount being retained on the

scaffolds (16.03 µg of heparin/per scaffold that is approximately 4.8 mm diameter by 5.8 mm high). Kim, *et al.* also used amine terminated PLGA scaffolds to immobilize heparin, but had an efficiency of 2.5%.[15]

5.4   BMP-2 Immobilization

As expected based on other published research [15, 35], BMP-2 was immobilized in greater quantities with scaffolds that had heparin covalently attached to the PLGA scaffolds using CDI than to any of the other BMP-2 attachment methods. However, it is not enough to have BMP-2 immobilized in greater quantities. If the immobilized protein is not oriented in a manner that is preferential for cell binding then the volume of BMP-2 attached is irrelevant because its ability to interact with cell surface receptors would be greatly reduced. Regardless, other studies have examined BMP-2 attachment on various scaffold types to verify the effects of BMP-2 on bone formation. It was worth comparing those results to the results obtained in this thesis research.

Kamakura, *et al.* randomly adsorbed 10 µg and 1 µg of rhBMP-2 to synthetic calcium phosphate granules that were used to form scaffolds for an *in vivo* experiment testing the effectiveness of their scaffolds for improving bone formation in critical size defects of rat calvarium.[70] There was no statistical difference in the effectiveness of the BMP-2 loaded scaffolds, but both cases were better at inducing bone growth than calcium phosphate scaffolds without BMP-2 loaded.

In a study by Boyan, *et al.*, PLGA particles with adsorbed BMP-2 were compared to demineralized freeze-dried bone allografts for bone formation at intramuscular sites in mice.[71] Here, 5 µg and 20 µg of BMP-2 loaded in PLGA particles showed 3.5-fold

and 4.4-fold increases in new bone area, respectively, when compared to the demineralized freeze-dried bone allograft.

Welch, *et al.* looked at absorbable collagen sponges with 0.86 mg of BMP-2 loaded into them to study the healing of critical size defects in large animal tibial fractures.[46] Again, the BMP-2 loaded vehicle resulted in enhanced bone volume in comparison to controls without BMP-2.

These experiments demonstrate that amounts as low as a microgram of BMP-2 are effective for promoting bone formation which suggests that the amounts of BMP-2 immobilized on our scaffolds should be sufficient to induce bone formation. However, none of the previously mentioned studies actually attached the BMP-2 on the biomaterial surface in any manner other than adsorption, and none addressed the issue of BMP-2 orientation.

Jeon, *et al.* investigated heparin loaded PLGA scaffolds as a method of providing a sustained delivery of BMP-2 for inducing ectopic bone formation. This study showed that scaffolds with heparin chemically attached to the scaffold surface prolonged the activity of BMP-2 *in vitro*.[15] However, no attempt was made to determine the orientation of the BMP-2 that was immobilized.

5.5   BMP-2 Orientation

The quantities of loaded or immobilized BMP-2 are important. However, for this research, efforts were also made to control and detect the orientation of the immobilized BMP-2 using heparin that was chemically attached and randomly adsorbed to PLGA scaffolds. Efforts to probe for the orientation of the immobilized BMP-2 involved the use of antibodies for the N- and C- terminus of BMP-2. These efforts were not without

difficulties. First, BMP-2 is a homodimer consisting of two, 114 amino acid sequence BMP-2 monomers. This suggests that there are two N- and C-terminals per BMP-2 molecule. Therefore, if only one of the BMP-2 N-terminals was bound to heparin, the other N-terminal was still available to bind with the antibody. Another difficulty associated with probing for orientation using the C-terminus antibody was that the C-terminus is buried somewhat within the structure of the molecule (Figure 2.3a) and will therefore be sterically hindered from binding with the C-terminus antibody.

With regards to the results of the antibody tests, the first thing noticed was the large error bars associated with high standard deviations. Not surprisingly, none of the differences were consider statistically significant. Some of the error was due to the inherent variations in the different scaffolds. Another source of the uncertainty was associated with steric hindrance affects on the antibodies used to probe for orientation of the BMP-2 molecule.

Assuming that the heparin does bind to the N-terminus region of BMP-2 [48], N-terminal antibody probes for BMP-2 should be more effective on scaffolds without heparin loaded and the C-terminal antibody probes should be more effective on scaffolds with heparin. Interestingly, neither the absolute values of absorbance nor the ratios of absorbance to BMP-2 mass supported this expectation. Again, the suspected reason for these results comes from the difficulties using antibodies and the variations in the scaffolds. However, the use of antibodies to probe for the conformation of the BMP-2 immobilized on the heparin loaded scaffolds did confirm that there was BMP-2 present. Also, the BMP-2 epitopes are still able to bind with the cell receptors and the

immobilization of BMP-2 using heparin did not alter the conformation such that the BMP-2 antibodies were ineffective at detecting BMP-2.

5.6   C3H10T1/2 Cells and BMP-2 Loaded Scaffolds

The results from the DNA assay (Table 4.6 and Figure 4.6a) seem to indicate that PLGA scaffolds by themselves (group 5) can support cell growth and proliferation. This was based on the DNA assay results that indicated more cell growth on blank PLGA scaffolds than on scaffolds with CDI activation. The results also indicated more cellular proliferation on the scaffolds that did not have CDI activation (groups 1 & 2) regardless of the presence of heparin. Based on the inverse relationship between proliferation and differentiation of osteoblastic cells,[72, 73] this was an indication that cells immobilized on the scaffolds with CDI activation (groups 3 & 4) were undergoing differentiation into the osteoblast phenotype more than they were proliferating on the scaffolds.

The results of the AP assay (Table 4.6 and Figure 4.6b) suggest that the oriented attachment of BMP-2 using heparin covalently bound to the scaffolds via CDI (group 3) does lead to more C3H10T1/2 differentiation than does random attachment of BMP-2. This was based on the differences in activity when comparing the oriented BMP-2 scaffolds from group 3 to those scaffolds that had BMP-2 randomly adsorbed without the use of heparin or CDI activation (group 2).

Another comparison that looked at the effectiveness of the different heparin immobilization methods on cellular differentiation suggests that BMP-2 bound to covalently attached heparin (group 3) was more effective at inducing C3H10T1/2 differentiation than does BMP-2 bound with the simple adsorption of heparin (group 1). The reason for this was likely due to the amount of BMP-2 immobilized on each scaffold

type. For instance, the amount of BMP-2 retained on scaffolds with covalently attached heparin was about three times greater than the amount of BMP-2 retained on scaffolds with adsorbed heparin (Figure 4.4). Similarly, the amount of AP activity from scaffolds with covalently attached heparin (group 3) was about three times greater than the activity of scaffolds with randomly attached heparin (group 1). The implication here was that heparin will orient BMP-2 in a preferred manner, but more heparin and therefore more oriented BMP-2 will be retained with covalent heparin attachment using CDI.

An argument can be made against the effectiveness of the covalently attached heparin method when compared to adsorbed heparin attachment though. The activity of each of the different BMP-2 immobilization methods was normalized by the amount of BMP-2 retained from a previous experiment (Table 4.6). The normalized AP activities were similar (16.0 for group 1 and 15.4 for group 3) and indicated that there was little difference in the amount of activity per μg of BMP-2 immobilized.

The other comparison of interest was the AP activity from scaffolds with covalently attached heparin using CDI (group 3) to scaffolds that had CDI activation without heparin (group 4). The activity from both cases was not statistically significant when compared to each other. These results suggest that CDI activation of the carboxyl groups can be as effective at immobilizing BMP-2 in a manner that promotes cell differentiation as can the oriented immobilization of BMP-2 using covalently attached heparin. However, the standard deviation was almost 50% with scaffolds that were CDI activated without heparin (group 4) compared to only ~13% with scaffolds that had CDI (covalently) attached heparin (group 3). This implies that while CDI activation alone can

lead to effective immobilization of BMP-2, it cannot do it as consistently as the scaffolds with covalently attached heparin.

Another observation was that about a third more BMP-2 was immobilized on covalently attached heparin scaffolds (group 3) than on CDI activated scaffolds with no heparin attachment (group 4) (Figure 4.4). Based on this observation, a comparison of the normalized AP activities between groups 3 and 4 was made. That comparison indicated that group 4 scaffolds actually induced more (23.9 versus 15.4 for normalized AP activity) differentiation of C3H10T1/2 cells than did the oriented BMP-2 scaffolds from group 3. This suggests that the CDI only scaffolds (group 4) had more activity with a smaller amount of BMP-2 and provides an argument against the effectiveness of orientation. However, there was nearly 50 % error associated with the group 4 scaffolds and neither the differences in the amounts of BMP-2 retained nor the AP activity associated with these two types of scaffolds was statistically significant. Also, before it can be concluded that oriented BMP-2 immobilization was no more effective at inducing osteoprogenitor cell differentiation than random immobilization, one must also consider the other effects of heparin. As mentioned in the background section, heparin has been shown to have an affinity for the N-terminus of BMP-2 which can be used to immobilize BMP-2 in a preferred orientation.[38, 48, 54] In addition, heparin has also been shown to prevent BMP-2 inhibitors such as noggin from binding with BMP-2 thereby increasing the activity of the immobilized BMP-2.[15, 45, 49, 62] The C3H10T1/2 in vitro system used for this research did not allow investigation of these effects. Regardless, this information suggests that while the immobilization of BMP-2 directly onto PLGA scaffolds may be as effective as at inducing differentiation *in vitro* than oriented

immobilization using heparin, it may not be effective in *in vivo* studies or even in *in vitro* studies with BMP-2 inhibitors present.

Results similar to those obtained in this research were obtained by another group. An *in vitro* study by Kim *et al.* showed that BMP-2 loaded onto heparin-conjugated PLGA scaffolds increased AP activity in osteoblasts for two weeks compared to only a transient three day increase with a decrease in activity thereafter for BMP-2 loaded onto unmodified (without heparin) PLGA scaffolds.[15] They reported that 19% of the BMP-2 was released from the heparin-conjugated scaffolds after 24 hours, whereas nearly all of the BMP-2 loaded onto the unmodified scaffolds was gone within 4 hours. A subsequent *in vivo* study also demonstrated more ectopic bone formation with BMP-2 loaded onto heparin-conjugated scaffolds than either BMP-2 loaded on unmodified scaffolds or heparin-conjugated scaffolds without the presence of BMP-2.[15] This further supports the use of heparin as an effective immobilization method for BMP-2. There was no mention in that study of determining the actual orientation of the BMP-2. Their goal was purely to determine if BMP-2 bound to covalently attached heparin produced more differentiation than BMP-2 loaded scaffolds without heparin.

6   CONCLUSION

The results indicated that PLGA scaffolds can be effectively constructed using PLGA microspheres. While these scaffolds were fabricated to be cylinders, the potential exists for the scaffolds to be shaped as desired to fit into any defect site.

The ability to chemically modify the surface of the scaffolds for the attachment of spacers was also demonstrated with the addition of both dihydrazides and heparin, although only heparin was used to attach BMP-2. The orientation of BMP-2 along with its distance from the biomaterial surface and its surface density has the potential to be controlled with the use of spacers. Also, the conclusion can be made that covalent heparin attachment using CDI chemistry will result in more heparin being retained and also more BMP-2 being immobilized on the scaffold surface.

With regards to the cellular activity, the scaffolds that had oriented BMP-2 attachment using covalently bound heparin demonstrated more activity on C3H10T1/2 cells than did both scaffolds with random adsorption of BMP-2 and scaffolds that had heparin simply adsorbed. Based on these results, it can be concluded that oriented immobilization can lead to increased cellular differentiation.

There was similar AP activity with both types of CDI activated scaffolds, that is with heparin as a spacer and with BMP-2 directly attached to the polymer. However, the scaffolds with randomly immobilized BMP-2 had much larger error associated with them than did the scaffolds that had BMP-2 oriented using covalently attached heparin. The conclusion here was that BMP-2 immobilized using CDI activation alone can lead to effective, but inconsistent, differentiation of C3H10T1/2 cells *in vitro* when compared to oriented immobilization using covalently bound heparin. It was also speculated that *in*

vivo studies would show that oriented immobilization of BMP-2 using covalent heparin attachment would show more effective osteoprogenitor differentiation than the random immobilization of BMP-2 (no heparin) scaffolds. This was due to the ability of heparin to prevent BMP-2 inhibitors from downregulating BMP-2. Future studies involving implantation of scaffolds in animals will be needed to further resolve this issue.

REFERENCES

1. Giannoudis, P.V., Dinopoulos, H., and Tsiridis, E. (2005). Bone substitutes: An update, *Injury* **36**:S20-S27.

2. Borden, M., El-Amin, S.F., Attawia, M., and Laurencin, C.T. (2003). Structural and human cellular assessment of a novel microsphere-based tissue engineered scaffold for bone repair, *Biomaterials* **24**:597-609.

3. Mooney, D.J., Boontheekul, T., Chen, R., and Leach, K. (2005). Actively regulating bioengineered tissue and organ formation, *Orthodontics & Craniofacial Research* **8**:141-144.

4. Hutmacher, D.W. (2000). Scaffolds in tissue engineering bone and cartilage, *Biomaterials* **21**:2529-2543.

5. Gunatillake, P. and Adhikari, R. (2003). Biodegradable synthetic polymers for yissue engineering, *European Cells & Materials Journal* **5**:1-16.

6. Borden, M., Attawia, M., Khan, Y., El-Amin, S.F., and Laurencin, C.T. (2004). Tissue-engineered bone formation in vivo using a novel sintered polymeric microsphere matrix, *J Bone Joint Surg Br* **86-B**:1200-1208.

7. Borden, M., Attawia, M., and Laurencin, C.T. (2002). The sintered microsphere matrix for bone tissue engineering: *In vitro* osteoconductivity studies, *Journal of Biomedical Materials Research* **61**:421-429.

8. Ratner, B.D., Hoffman, A.S., Schoen, F.J., and Lemons, J.E. (2003). *Biomaterials Science: An Introduction to Materials in Medicine*. 2nd ed. San Diego: Academic Press.

9. Tabata, Y. (2005). Significance of release technology in tissue engineering, *Drug Discovery Today* **10**:1639-1646.

10. Hsiong, S.X. and Mooney, D.J. (2006). Regeneration of vascularized bone, *Periodontology 2000* **41**:109-122.

11. Park, Y.J., Kim, K.H., Lee, J.Y., Ku, Y., Lee, S.J., Min, B.M., and Chung, C.P. (2006). Immobilization of bone morphogenetic protein-2 on a nanofibrous chitosan membrane for enhanced guided bone regeneration, *Biotechnol. Appl. Biochem.* **43**:17-24.

12. Engelberg, I. and Kohn, J. (1991). Physico-mechanical properties of degradable polymers used in medical applications: A comparative study, *Biomaterials* **12**:292-304.

13. (2006). Product catalog, 2006, www.polysciences.com.

14. Jun Jin Yoon, T.G.P. (2001). Degradation behaviors of biodegradable macroporous scaffolds prepared by gas foaming of effervescent salts, *Journal of Biomedical Materials Research* **55**:401-408.

15. Jeon, O., Song, S.J., Kang, S.-W., Putnam, A.J., and Kim, B.-S. (2007). Enhancement of ectopic bone formation by bone morphogenetic protein-2 released from a heparin-conjugated poly(l-lactic-co-glycolic acid) scaffold, *Biomaterials* **28**:2763-2771.

16. Chung, H., Kim, H., Yoon, J., and Park, T. (2006). Heparin immobilized porous PLGA microspheres for angiogenic growth factor delivery, *Pharmaceutical Research* **23**:1835-1841.

17. Yoon, J.J., Chung, H.J., Lee, H.J., and Park, T.G. (2006). Heparin-immobilized biodegradable scaffolds for local and sustained release of angiogenic growth factor, *Journal of Biomedical Materials Research* **79A**:934-942.

18. Junchuan, Z., Hong, Z., Linbo, W., and Jiandong, D. (2006). Fabrication of three dimensional polymeric scaffolds with spherical pores, *Journal of Materials Science* **41**:1725-1731.

19. Lee, C.-T. and Lee, Y.-D. (2006). Preparation of porous biodegradable poly(lactide-co-glycolide)/ hyaluronic acid blend scaffolds: Characterization, in vitro cells culture and degradation behaviors, *Journal of Materials Science: Materials in Medicine* **17**:1411-1420.

20. Ren, T., Ren, J., Jia, X., and Pan, K. (2005). The bone formation *in vitro* and mandibular defect repair using PLGA porous scaffolds, *Journal of Biomedical Materials Research* **74A**:562-569.

21. Kim, H.K., Chung, H.J., and Park, T.G. (2006). Biodegradable polymeric microspheres with "open/closed" pores for sustained release of human growth hormone, *Journal of Controlled Release* **112**:167-174.

22. Yoon, J.J., Kim, J.H., and Park, T.G. (2003). Dexamethasone-releasing biodegradable polymer scaffolds fabricated by a gas-foaming/salt-leaching method, *Biomaterials* **24**:2323-2329.

23. Wu, L., Jing, D., and Ding, J. (2006). A "room-temperature" injection molding/particulate leaching approach for fabrication of biodegradable three-dimensional porous scaffolds, *Biomaterials* **27**:185-191.

24. Hulbert, S.F., Young, F.A., Mathews, R.S., Klawitter, J.J., Talbert, C.D., and Stelling, F.H. (1970). Potential of ceramic materials as permanently implantable skeletal prostheses, *Journal of Biomedical Materials Research* **4**:433-456.

25. Li, R.H. and Wozney, J.M. (2001). Delivering on the promise of bone morphogenetic proteins, *Trends in Biotechnology* **19**:255-265.

26. Winn, S.R., Hu, Y., Sfeir, C., and Hollinger, J.O. (2000). Gene therapy approaches for modulating bone regeneration, *Advanced Drug Delivery Reviews* **42**:121-138.

27. Kirker-Head, C.A. (2000). Potential applications and delivery strategies for bone morphogenetic proteins, *Advanced Drug Delivery Reviews* **43**:65-92.

28. Lind, M., Overgaard, S., Ongpipattanakul, B., Nguyen, T., Bunger, C., and Soballe, K. (1996). Transforming growth factor-β_1 stimulates bone ongrowth to weight-loaded tricalcium phosphate coated implants: An experimental study in dogs, *J Bone Joint Surg Br* **78-B**:377-382.

29. Piattelli, A., Scarano, A., Corigliano, M., and Piattelli, M. (1996). Effects of alkaline phosphatase on bone healing around plasma-sprayed titanium implants: a pilot study in rabbits, *Biomaterials* **17**:1443-1449.

30. Massia, S.P. and Hubbell, J.A. (1990). Convalent surface immobilization of Arg-Gly-Asp- and Tyr-Ile-Gly-Ser-Arg-containing peptides to obtain well-defined cell-adhesive substrates, *Analytical Biochemistry* **187**:292-301.

31. Dee, K.C., Rueger, D.C., Andersen, T.T., and Bizios, R. (1996). Conditions which promote mineralization at the bone-implant interface: a model in vitro study, *Biomaterials* **17**:209-215.

32. Maheshwari, G., Brown, G., Lauffenburger, D.A., Wells, A., and Griffith, L.G. (2000). Cell adhesion and motility depend on nanoscale RGD clustering, *J Cell Sci* **113**:1677-1686.

33. Dee, K.C., Andersen, T.T., and Bizios, R. (1998). Design and function of novel osteoblast-adhesive peptides for chemical modification of biomaterials, *Journal of Biomedical Materials Research* **40**:371-377.

34. Rezania, A. and Healy, K.E. (1999). Biomimetic peptide surfaces that regulate adhesion, spreading, cytoskeletal organization, and mineralization of the matrix deposited by osteoblast-like cells, *Biotechnol. Prog.* **15**:19-32.

35. Takada, T., Katagiri, T., Ifuku, M., Morimura, N., Kobayashi, M., Hasegawa, K., Ogamo, A., and Kamijo, R. (2003). Sulfated polysaccharides enhance the biological activities of bone morphogenetic proteins, *J. Biol. Chem.* **278**:43229-43235.

36. Groeneveld, E.H. and Burger, E.H. (2000). Bone morphogenetic proteins in human bone regeneration, *Eur J Endocrinol* **142**:9-21.

37. Urist, M.R. (1965). Bone: formation by autoinduction, *Science* **150**:893-899.

38. Scheufler, C., Sebald, W., and Hulsmeyer, M. (1999). Crystal structure of human bone morphogenetic protein-2 at 2.7 A resolution, *Journal of Molecular Biology* **287**:103-115.

39. Wozney, J.M. (1989). Bone Morphogenetic Proteins, *Progress in Growth Factor Research* **1**:267-280.

40. Kim, K.J., Itoh, T., and Kotake, S. (1997). Effects of recombinant human bone morphogenetic protein-2 on human bone marrow cells cultured with various biomaterials, *Journal of Biomedical Materials Research* **35**:279-285.

41. Kubota, K., Iseki, S., Kuroda, S., Oida, S., Iimura, T., Duarte, W.R., Ohya, K., Ishikawa, I., and Kasugai, S. (2002). Synergistic effect of fibroblast growth factor-4 in ectopic bone formation induced by bone morphogenetic protein-2, *Bone* **31**:465-471.

42. Lind, M., Eriksen, E.F., and Bunger, C. (1996). Bone morphogenetic protein-2 but not bone morphogenetic protein-4 and -6 stimulates chemotactic migration of human osteoblasts, human marrow osteoblasts, and U2-OS cells, *Bone* **18**:53-57.

43. Wozney, J.M. and Rosen, V. (1998). Bone morphogenetic protein and bone morphogenetic protein gene family in bone formation and repair, *Clinical Orthopaedics and Related Research* **346**:26-37.

44. Zegzula, H.D., Buck, D.C., Brekke, J., Wozney, J.M., and Hollinger, J.O. (1997). Bone Formation with Use of rhBMP-2 (Recombinant Human Bone Morphogenetic Protein-2), *J Bone Joint Surg Am* **79**:1778-1790.

45. Zhao, B., Katagiri, T., Toyoda, H., Takada, T., Yanai, T., Fukuda, T., Chung, U.-i., Koike, T., Takaoka, K., and Kamijo, R. (2006). Heparin potentiates the *in vivo* ectopic bone formation induced by bone morphogenetic protein-2, *J. Biol. Chem.* **281**:23246-23253.

46. Welch, R.D., Jones, A.L., Bucholz, R.W., Reinert, C.M., Tjia, J.S., Pierce, W.A., Wozney, J.M., and Li, X.J. (1998). Effect of recombinant human bone morphogenetic protein-2 on fracture healing in a goat tibial fracture model, *Journal of Bone and Mineral Research* **13**:1483-1490.

47. John, M.W. (1992). The bone morphogenetic protein family and osteogenesis, *Molecular Reproduction and Development* **32**:160-167.

48. Ruppert, R., Hoffmann, E., and Sebald, W. (1996). Human bone morphogenetic protein 2 contains a heparin-binding site which modifies its biological activity, *European Journal of Biochemistry* **237**:295-302.

49. Chen, D., Zhao, M., and Mundy, G.R. (2004). Bone Morphogenetic Proteins, *Growth Factors* **22**:233-241.

50. Kirsch, T., Nickel, J., and Sebald, W. (2000). BMP-2 antagonists emerge from alterations in the low-affinity binding epitope for receptor BMPR-II, *European Molecular Biology Organization* **19**:3314-3324.

51. Kirsch, T., Sebald, W., and Dreyer, M.K. (2000). Crystal structure of the BMP-2?BRIA ectodomain complex, *Nature Structural Biology* **7**:492.

52. Keller, S., Nickel, J., Jin-Li, Z., Sebald, W., and Mueller, T.D. (2004). Molecular recognition of BMP-2 and BMP receptor IA, *Nature Structural & Molecular Biology* **11**:481-488.

53. Nickel, J., Dreyer, M.K., Kirsch, T., and Sebald, W. (2001). The crystal structure of the BMP-2:BMPR-IA complex and the generation of BMP-2 antagonists, *J Bone Joint Surg, Am* **83**:S1-7.

54. Koenig, B.B., Cook, J.S., Wolsing, D.H., Ting, J., Tiesman, J.P., Correa, P.E., Olson, C.A., Pecquet, A.L., Ventura, F., and Grant, R.A. (1994). Characterization and cloning of a receptor for BMP-2 and BMP-4 from NIH 3T3 cells, *Mol. Cell. Biol.* **14**:5961-5974.

55. Mace, P.D., Cutfield, J.F., and Cutfield, S.M. (2006). High resolution structures of the bone morphogenetic protein type II receptor in two crystal forms: Implications for ligand binding, *Biochemical and Biophysical Research Communications* **351**:831-838.

56. Griffith, L.G. and Lopina, S. (1998). Microdistribution of substratum-bound ligands affects cell function: hepatocyte spreading on PEO-tethered galactose, *Biomaterials* **19**:979-986.

57. Schense, J.C. and Hubbell, J.A. (2000). Three-dimensional migration of neurites Is mediated by adhesion site density and affinity, *J. Biol. Chem.* **275**:6813-6818.

58. Naumann, M., Reuter, R., Metz, P., and Kopperschlager, G. (1989). Affinity chromatography of bovine heart lactate dehydrogenase using dye ligands linked directly or spacer-mediated to bead cellulose, *Journal of Chromatography A* **466**:319-329.

59. Itoyama, K., Tanibe, H., Hayashi, T., and Ikada, Y. (1994). Spacer effects on enzymatic activity of papain immobilized onto porous chitosan beads, *Biomaterials* **15**:107-112.

60. Hermanson, G.T. (1996). *Bioconjugate Techniques*. San Diego: Academic Press.

61. Irie, A., Habuchi, H., Kimata, K., and Sanai, Y. (2003). Heparan sulfate is required for bone morphogenetic protein-7 signaling, *Biochemical and Biophysical Research Communications* **308**:858-865.

62. Paine-Saunders, S., Viviano, B.L., Economides, A.N., and Saunders, S. (2002). Heparan sulfate proteoglycans retain noggin at the cell surface. A potential mechanism for shaping bone morphogenetic protein gradients, *J. Biol. Chem.* **277**:2089-2096.

63. Liu, L.-S., Ng, C.-K., Thompson, A.Y., Poser, J.W., and Spiro, R.C. (2002). Hyaluronate-heparin conjugate gels for the delivery of basic fibroblast growth factor (FGF-2), *Journal of Biomedical Materials Research* **62**:128-135.

64. Brooks, K.A., Allen, J.R., Feldhoff, P.W., and Bachas, L.G. (1996). Effect of surface-attached heparin on the response of potassium-selective electrodes, *Analytical Chemistry* **68**:1439-1443.

65. Smith, P.K., Mallia, A.K., and Hermanson, G.T. (1980). Colorimetric method for the assay of heparin content in immobilized heparin preparations, *Analytical Biochemistry* **109**:466-473.

66. Yoon, J.J. and Park, T.G. (2001). Degradation behaviors of biodegradable macroporous scaffolds prepared by gas foaming of effervescent salts, *Journal of Biomedical Materials Research* **55**:401-408.

67. Li, J., Li, S., Blitterswijk, C., and Groot, K. (2006). Cancellous bone from porous Ti6Al4V by multiple coating technique, *Journal of Materials Science: Materials in Medicine* **17**:179-185.

68. Sevilla, P., Aparicio, C., Planell, J.A., and Gil, F.J. (2007). Comparison of the mechanical properties between tantalum and nickel-titanium foams implant materials for bone ingrowth applications, *Journal of Alloys and Compounds* **439**:67-73.

69. Gittens, S.A., Bagnall, K., Matyas, J.R., Lobenberg, R., and Uludag, H. (2004). Imparting bone mineral affinity to osteogenic proteins through heparin-bisphosphonate conjugates, *Journal of Controlled Release* **98**:255-268.

70. Kamakura, S., Nakajo, S., Suzuki, O., and Sasano, Y. (2004). New scaffold for recombinant human bone morphogenetic protein-2, *Journal of Biomedical Materials Research* **71A**:299-307.

71. Boyan, B.D., Lohmann, C.H., Somers, A., Niederauer, G.G., Wozney, J.M., D., D.D., Carnes, J., D. L., and Schwartz, Z. (1999). Potential of porous poly-D,L-lactide-co-glycolide particles as a carrier for recombinant human bone morphogenetic protein-2 during osteoinduction *in vivo*, *Journal of Biomedical Materials Research* **46**:51-59.

72. Pockwinse, S.M., Wilming, L.G., Conlon, D.M., Stein, G.S., and Lian, J.B. (1992). Expression of cell growth and bone specific genes at single cell resolution during development of bone tissue-like organization in primary osteoblast cultures, *Journal of Cellular Biochemistry* **49**:310-323.

73. Stein, G.S., Lian, J.B., and Owen, T.A. (1990). Relationship of cell growth to the regulation of tissue-specific gene expression during osteoblast differentiation, *FASEB J.* **4**:3111-3123.

VITA

Randy Hilliard was born in December 1968 in Grove, OK. He obtained his Associates of Science from Jefferson Community College in Louisville, KY in 1995 and his Bachelors of Arts in Chemistry from the University of Kentucky in 1997. He began the masters program in the Center for Biomedical Engineering at the University of Kentucky in 2005. While attending the Center for Biomedical Engineering, he presented a poster at the 2007 Society for Biomaterials annual meeting. He also served as the president of the UK chapter of the Biomedical Engineering Society. Before attending school to obtain his master's degree, Randy served as a Communications and Information Systems Officer in the United States Air Force, achieving the rank of Captain. He served in Operation Desert Shield/Storm and Operation Enduring Freedom in Afghanistan while in the military and was named the 2001 Air Force Special Operations Communications and Information Systems Officer of the Year.